6-24-2014

Chemically Modified Proteins as Highly Stable Building Blocks For Functional Bionanomaterials

Marc J. Novak
marc.novak15@gmail.com

Chemically Modified Proteins as Highly Stable Building Blocks For Functional Bionanomaterials

Marc Joseph Novak

B.S. Molecular & Cell Biology
University of Connecticut, 2012

A Thesis

Submitted in Partial Fulfillment of the

Requirements for the Degree of

Master of Science

At the

University of Connecticut

2014

APPROVAL PAGE

Masters of Science Thesis

Chemically Modified Proteins as Highly Stable Building Blocks For Functional Bionanomaterials

Presented by

Marc Joseph Novak, B.S.

Major Advisor_____
Dr. Challa V. Kumar

Associate Advisor_____
Dr. Carolyn M. Teschke

Associate Advisor_____
Dr. Victoria L. Robinson

University of Connecticut

2014

Table of Contents

List of Tables

List of Figures

Figure 1.8. Thermal inactivation of GOx based on activity retention of native and modified GOx derivaties. Samples were stored at above displayed temperatures for 15 minutes, then immediately cooled to 4 °C. After cooling period, samples were equilibrated to room temperature in order to measure activity at constant temperature.

Figure 2.1. Interaction of 4 μM GOx derivatives to 0.15 mg/mL GO in 10 mM sodium phosphate buffer as measured by (**A**) equilibrium binding studies and (**B**) changes in the zeta potential upon binding.

Figure 2.2. Transmission electron microscopy micrographs of 4 μM GOx(0) bound to 0.15 mg/mL GO nano sheets in deionized water. Panel A shows intercalation of dark protein clusters within multiple stacked GO sheets. Panels B & C denote high protein surface coverage of normally smooth, glassy surface of GO to create irregular, gritty surface of GO/GOx conjugates.

Figure 2.3. Retention of (**A**) the protein secondary structure, and (**B**) correlation of the retention of enzymatic activities (squares) with the retention of the secondary structure (diamonds) of modified GOx/GO (4 μM protein, 0.15 mg/mL GO) as a function of charge on the GOx derivative. Solid blue line denotes structure and activity measurements of unmodified GOx under same conditions of pH and iconic strength.

Figure 2.4. (**A**) Comparison of activities of 1 μM GOx (black line) and GO/GOx samples. (**B**) Percentage activity retention of GO/GOx derivatives based on charge relative to native GOx. All activities were taken at room temperature in 10 mM phosphate buffer pH 7.0. Color scheme of samples matches that described in **Figure 2.3**.

Figure 2.5: Thermal stability studies of 4 μM GOx derivatives (A) and 4μM GOx derivatives bound to 0.15 mg/mL GO (B) in 10 mM phosphate buffer, pH 7.0. Activity retention based on initial rate after 15 minute incubation time at denoted temperature is recorded. All samples were immediately cooled to an internal temperature of 4 °C then re-equilibrated to room temperature to perform all activity studies under same overall temperature after heating.

Figure 2.6. Plots of specific activities of GOx charge derivatives bound to GO relative to initial activity of GO/GOx derivative as a function of storage time in days. 4 μM PCM GOx in 10 mM phosphate buffer at pH 7.0 were stored in absence of substrate with and without 0.15 mg/mL GO at 40 °C. Aliquots were taken periodically, equilibrated to room temperature, and activity was measured in triplicate. Initial rates for each derivative were averaged and relative activity to the initial measurement before incubation was compared.

Figure 2.7. Half-life versus charge of PCM GOx derivatives (4 μM protein, black line) and GO/GOx derivatives (4 μM protein, 0.15 mg/ml GO, red line). GO/GOx(35) displayed >150 times increase in half-life at 40 °C when compared to that of unmodified, unbound GOx maintained under identical conditions.

Figure 2.8. Chemical stability of 4 μM GOx (black) and chemically modified GOx derivatives (red), (solid lines) compared with equal concentration of enzymes reacted with 0.15 mg/mL GO (dashed lines) at pH 7 under increasing molar concentration of guanidine hydrochloride. Increased favorability in electrostatic binding to GO surface did not enhance stability under denaturing conditions to a significant extent.

Figure 2.9: GO/GOx conjugates stored for 24 hours at room temperature. Major precipitation was noted for samples 7 (GOx (66)) and 8 (GOx (78)), while all others remained as stable suspensions. Sample numbers correspond to those in **Table 2.1**.

Figure 2.10. (**A**) Extensive retention of the secondary structure of GO/GOx(0) (4 μM protein,0.15 mg/ml GO) when compared to its initial CD signal. CD intensities of GO/GOx derivatives at 222 nm as a function of enzyme charge after 40 days, maintained at 40˚C (blue) *vs* their corresponding original values before incubation (red). All samples were stored in the absence of substrate in 10 mM phosphate buffer, pH 7.0. (**B**) Superimposition of the CD of GO/GOx (0) and GO/GOx (35) before (solid lines) and after 33 days at 40 °C of half-life studies (dashed lines)to show comparison of structure retention.

Figure 3.2. Zeta Potential measurement of 300 μM BSA_{TETA} in solution at pH 7.0 in 10 mM Phosphate buffer. Addition of triethylenetetramine functional groups via an amide bond after EDC chemistry reaction change net charge of protein molecules to ~24.5 from a native charge of ~ -30.

Figure 3.3. Optical microscopy of interaction of 300 μM BSA_{TETA}/ 800 μM fsDNA dissolved in HPLC grade dH_2O casted onto class cover slip and dried over-night at room temperature. Highly organized structures can be observed on mm length scale with exceptional uniformity from both 100x (**A**) and 400x (**B**) magnification.

Figure 3.4. Scanning electron microscopy (SEM) micrographs of 300 μM BSA_{TETA}/ 800 μM fsDNA dissolved in HPLC grade dH_2O, drop-casted onto glass cover slip and dried at room temperature overnight. High degree of organization and uniformity that was observed in optical microscopy also apparent on scale of hundreds (**A**) and tens of microns (**B**). Surface morphology (**C**) also appears to demonstrate multitude of molecular structures organized in single linear fashion.

Figure 3.5. SEM micrographs of 300 μM BSATETA (A) and 800 μM fsDNA (B) dissolved in HPLC grade DI and drop casted onto glass cover slip. Samples were air dried overnight in laboratory fume hood at room temperature before coating with gold-palladium for analysis.

Figure 3.6. Elemental analysis of 300 μM combined with 800 μM fsDNA in HPLC grade dH_2O (**A**, **B**) displaying composition of molecular assemblies is in fact combination of biological polymer components carbon (**C**), oxygen (**D**), nitrogen (**E**), and phosphorous (**F**). No discernable order of elements is visible at the high magnification, leading to belief that protein-DNA binding is random at molecular level.

Figure 3.7. Atomic Force microscopy (AFM) of individual BSA_{TETA}/fsDNA molecular assembly fibers (300 μM BSA_{TETA}, 800 μM fsDNA) extracted from glass cover slip after drying 24 hours at room temperature. Samples were placed on mica surface and measured at scan rate of 0.1 Hz.

Figure 3.8. AFM micrograph of surface composition of BSA_{TETA}/fsDNA construct zoomed in to analyze fibril-like structures appearing to line surface. Distinct linear fibers corresponding to the lengthwise orientation of larger superstructures can be distinguished.

Figure 3.9: AFM micrograph and 2-dimensional profile of enhanced surface morphology of BSA_{TETA}/ fsDNA constructs consisting of dozens of microfibrils with high uniformity and width of ~1.5 μm.

Figure 3.10. Powder X-Ray Diffraction data of molecular assembly when compared with glass slide surface which 300 μM BSA_{TETA}/ 800 μM DNA dissolved in HPLC grade dH_2O was drop casted on. Data suggests that while molecular assemblies are highly organized on micron scale, there is no discernable ordering or stacking of organized micro-scale structures which compose larger highly organized structures.

List of Schemes

Chapter 1

Chemical Modification of Glucose Oxidase for Improved Solution Stability

1.1 Introduction

Proteins, especially enzymes, are important molecular machines that can act as catalysts in numerous biological and chemical processes by stabilizing the transition state between reactants and products in addition to lowering the activation energy of reaction.[1,2] However, a limiting property of most natural proteins and enzymes is that they are unstable in solution due to sensitivity to conditions including temperature, pH, and ionic strength.[3,4,5] When these conditions are optimized, enzyme folding leads to the most stable conformation, burying non-polar residues and exposing charged regions of the polar solvent.[6] How these charged residues are arranged under physiological conditions can affect overall stability of a protein due to electrostatic strain of like-charged residues in close proximity to one another. Proteins with highly positive or negative net charges at physiological pH have the potential to favor the unfolded state due to charge-charge repulsion energy and unfavorable coulombic strain that could contribute substantially to the denaturation free energy.[7,8]

Attempts to stabilize proteins have been conducted by the use of additives and genetic mutational approaches, but each of these experimental methods has particular draw-backs that make the process of improving protein stability difficult. Mutational approaches produce limited quantities of correctly modified product and cannot be regarded as readily scalable.[9] Recent studies into site-directed mutations of loops and turns to improve lipase stability and prevent its aggregation show that the protein surface plays a very important role in controlling protein stability.[10,11,12] However, there is a considerable challenge in identifying which residues are necessary to be selectively mutated to produce the most stable conformations, leading to the possibility of the mutant protein not folding into its correct, biologically active form.[13] The use of additives to improve stability is also popular, but removal of the additives prior to use of the

enzyme is required and leads to difficulty interpreting which additives or combinations of additives would stabilize a specific enzyme.[14]

When compared with the aforementioned techniques, chemical modification is a convenient and robust approach to modify specific physical, chemical, and biological properties of proteins.[15,16,17] In addition, chemical modification provides a unique opportunity to control molecular level behavior of biocatalysts and functionalize them for various applications.[18,19,20,21,22, 23, 24] Surface residues of enzymes have been chemically modified to facilitate the formation of novel enzyme-enzyme, enzyme-DNA, and enzyme-polymer complexes with varying degrees of improved function and stability.[25, 26, 27, 28, 29, 30] In addition, chemically modified enzymes are being utilized in gene delivery, biocatalysis, and development of functional biomaterials.

Here, we have theorized that by using a systematic approach to alter the surface charge from a highly negative charge density to a more neutral charge, protein stability is increased due to stabilization of the folded state. This can be achieved by increasing the enzyme-water interface interaction as well as lowering the coloumbic strain that arises from negative charge-charge repulsion. To test this hypothesis, glucose oxidase[31] (GOx) was chosen as a model system. GOx is a homodimeric glycoprotein which utilizes molecular oxygen to oxidize β-D-glucose to gluconic acid via the FAD cofactor associated with the active site of the enzyme. With a total of 126 carboxyl functional groups and a net charge of -65 units at pH 7.0, this protein has a significantly high negative charge desnity at physiological pH. GOx is widely used in the food industries, fabrication of glucose sensors, and development of fuel cells.[32] However, the usefulness of GOx as a functional biomaterial is hindered by its thermal and kinetic instability under taxing conditions. Improvements in stability in order to increase this enzyme's

industrial application while retaining biocatalytic activity is a major challenge that we address with this work.

Enzyme net charge alteration is achieved by systematically converting GOx carboxylate functional groups to amides (Scheme 1) using a versatile group of amines varying in charge, length, and flexibility. After modification, stabilities of modified GOx derivatives were measured as a function of its modified charge when compared to that of native, unmodified GOx. Solution stability of the proteins was monitored by comparing the half-life of native GOx to that of the modified GOx samples. Controlled chemical manipulation under regulated conditions reduced the net charge of GOx by replacing the negatively charged carboxyl croups with charge-neutral amide functions that carry with them the possibility of additional charges after interaction with the protein.

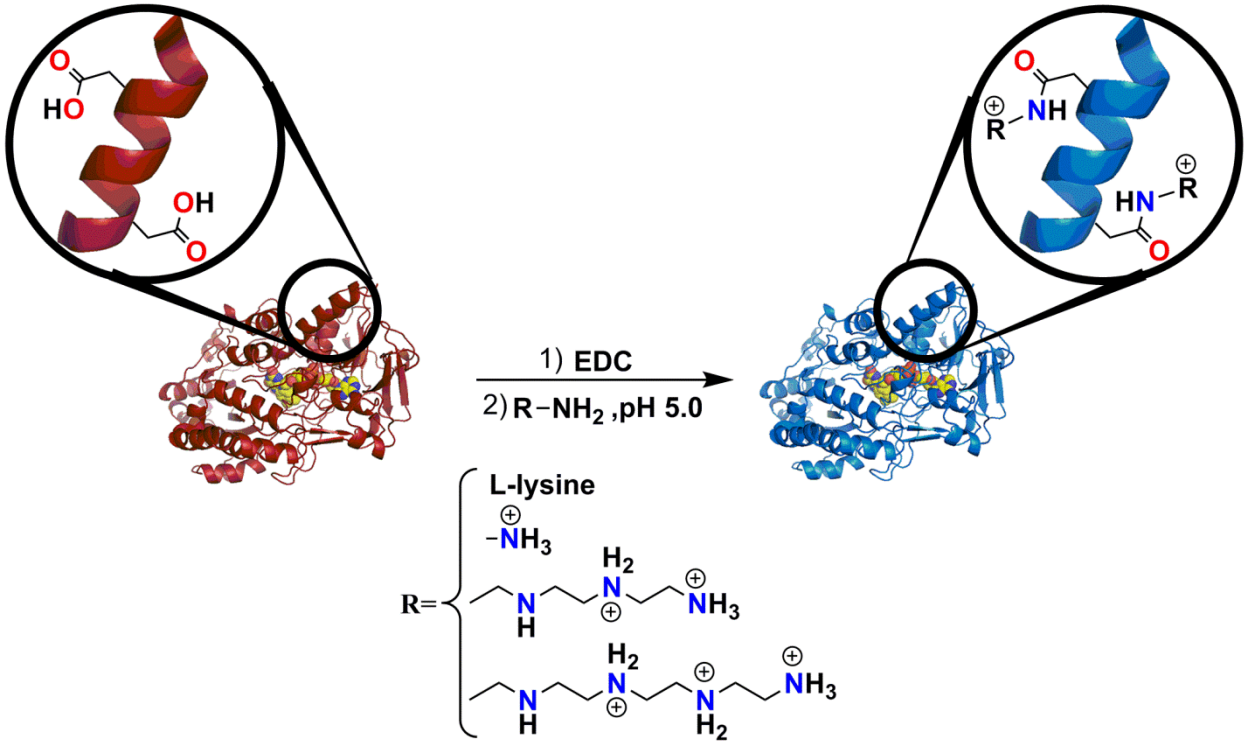

Scheme 1.1. Chemical modification of GOx carboxylate functional groups using L-lysine, ammonium chloride, triethylenetetramine (TETA), or tetraethylenepentamine (TEPA). Alteration of carboxyl groups into amide groups is performed using EDC chemistry in a non-site-specific technique.

Amidation of GOx carboxyl groups was carried out by reaction with L-Lysine, ammonium chloride, Triethylenetetramine (TETA), and Tetraethylenepentamine (TEPA) facilitated by carbodiimide chemistry to produce corresponding amide groups. In addition to formation of the initial amide bond, TETA and TEPA provide additional basic sites for further side chain protonation, leading to the potential for additional reduction of enzyme negative charge. The reaction conditions, such as the amine concentration and pH, are adjusted such that a distinguishable GOx charge ladder is produced. Controlled carboxyl modification, therefore, can lower the net negative charge on the enzyme while decorating the surface with strongly polar amide groups. Carboxyl-modified glucose oxidase derivatives showed increased stability, which correlated directly with the extent of GOx charge reduction.

1.2 Experimental

1.2.1 Chemicals and Materials

Glucose oxidase (GOx) from *Aspergillus niger*, L-Lysine, Ammonium Chloride (NH_4Cl), Triethylenetetramine (TETA), Tetraethylenepentamine (TEPA), D-(+)- glucose, Guaiacol, Graphite, and sodium phosphate dibasic (Na_2HPO_4) were purchased from Sigma-Aldrich Co. (St. Louis, MO). Horseradish Root Peroxidase (HRP) was purchased from Calzyme Laboratories, Inc. (San Luis Obispo, CA). N-(3-dimethlaminopropyl)-N-ethylcarbodiimide (EDC) was purchased from TCI America (Portland, OR). Protein samples were prepared in the respective buffers used for synthesis, as indicated, and the concentration determined from the absorbance of GOx using molar extinction co-efficient of 267,000 $M^{-1}cm^{-1}$ at 280nm or 28,200 $M^{-1}cm^{-1}$ at 450nm (FAD cofactor).

1.2.2 Chemical Modification of GOx

Surface groups of GOx were modified by reacting the carboxyl functional groups of enzymes with appropriate amines, by adopting reported procedures.[33] 6 mL of GOx stock (5 mg/ml) in deionized water (DI), 200 μL of 0.5 M TETA stock, pH adjusted 5.5, and 3.8 mL of DI were added to a reaction vial and stirred for 30 minutes. After the equilibration phase of amine and protein, 100 μL of 0.5 M EDC stock was added drop wise with 10-15 second intervals, while the reaction stirred at 550 rpm. After 15 minutes, the mixture was stirred at 250 rpm for four hours at room temperature and unreacted EDC, TETA, and other byproducts of synthesis were removed by 3 rounds of dialysis against 1 L of 10mM phosphate buffer (Na_2HPO_4) using 25 kDa molecular weight cut-off dialysis membrane from Spectrum Laboratories, Inc. (Rancho Dominguez, CA). This approach was also used for enzyme

modification with other amines. The degree of modification was carefully controlled by adjusting EDC and amine concentration, pH of the reaction mixture, enzyme concentration and the reaction time until all GOx has been reacted to form the modified enzyme. These details are collected and presented in **Table 1.1.** Modified enzymes were examined by agarose gel electrophoresis,[34] and SDS PAGE,[35] for purity, extent of charge modification, and for the presence of any cross-linked products.

1.2.3 Agarose Gel Electrophoresis

Native agarose gel electrophoresis was performed using horizontal gel electrophoresis apparatus (Gibco model 200, Life Technologies Inc, MD). Molecular biology grade agarose from U.S. Biological (Swampscott, MA) (0.5% w/v), in 40 mM Tris-acetate buffer, pH 7.0, was dissolved via heating and then poured into gel apparatus to form casted gel. 8μL of modified GOx samples were combined with 17 μL loading buffer (50% v/v glycerol and 0.01% w/w bromophenol blue) and 20 μL of samples were loaded into wells at the middle of the gel so that they could migrate toward the negative or positive electrode, depending on the net charge of the enzyme. Running buffer used for all the samples was 40 mM Tris-acetate, pH 7. Potential of 100 V was applied for approximately 30 minutes at room temperature. Gels were stained overnight with 10% v/v acetic acid, 0.02% w/w Coomassie blue, and destained in 10% v/v acetic acid, overnight. Gels were photographed using a BioRad Molecular Imager Gel Doc XRS System.

Table 1.1 Reaction conditions used for the bioconjugate preparation. Optimized concentrations of amines (mM) and enzymes (3 mg/ml) (pH 4.5- 5.2) in Na_2HPO_4 (10 mM), at 25 ^{0}C. Reaction stirred for 4 hours after addition of EDC.

Bioconjugate Sample	**Amine Concentration-Synthesis**	**Amine/ Reaction pH**	**Lane Number (Figures 1.1. & 1.2.)**
Glucose Oxidase (GOx)	---	5.0	1
GOx (-44)	5 mM TEPA	5.0	2
GOx (-32)	50 mM L-lysine	4.5	3
GOx (-18)	100 mM NH_4Cl	5.0	4
GOx (0)	10 mM TETA	5.2	5
GOx (35)	20 mM TETA	5.2	6
GOx (66)	50 mM TETA	5.2	7
GOx (78)	70 mM TEPA	5.2	8

1.2.4 SDS-PAGE:

The purity and the presence of cross-linked products of the modified enzyme was also assessed using SDS-PAGE by following a reported method. After synthesis and dialysis, modified enzyme samples were completely dried in a SpeedVac (Savant Speedvac concentrator, Savant Inc, NY) for 2 hours, and 24 µl of loading buffer (SDS (7% v/v), glycerol (13% v/v), Tris-HCl (50 mM), β-mercaptoethanol (2 % v/v) and bromophenol blue (0.15% v/v) pH 6.8), was added. The mixture was heated for 60 seconds in boiling water and loaded (8 µl) into 9% acrylamide gel containing separating and stacking gels. The separating gel contained acrylamide, gel buffer, 80% glycerol, 10% ammonium per sulfate (APS) and TEMED (N, N, N, N-tetramethylethylenediamine) and deionized water. Stacking gel contained acrylamide, gel buffer, deionized water, 10% APS and TEMED. Potential of 100 V was applied until the dye passed through the stacking gel and after that the potential increased to 150 V for an additional 2 h. Gel was first stained for 1 h with stain I (one) which contained 20% v/v 2-propanol, 20% v/v acetic acid, 0.02% w/w Coomassie Blue and staining was continued with stain II (two) which contained 20% v/v acetic acid. 0.02% w/w Coomassie Blue for additional 24 h. Gels were then destained in 10% acetic acid for 24 h and imaged using BioRad Molecular Imager Gel Doc XRS System.

1.2.5 Charge Analysis of Modified GOx Samples

Using the known isoelectric point (4.6) and charge (-65) of native glucose oxidase at pH 7, charge of modified samples was able to be determined. The gel was photographed using a Molecular Imager Gel Doc XR System and resulting photograph was analyzed using NIH ImageJ v1.47 software (National Institute of Health, U.S.A.). Migration distance of unmodified GOx was used as a standard to quantify charge of modified samples based on distance traveled to

either the positive or negative electrode. Since addition of amine sidechains was shown by SDS-PAGE to not affect size of the protein to a considerable extent, the migration of the proteins is presumed to be due to its net charge.

1.2.6 Circular Dichroism (CD) Studies

The CD spectra were recorded on a JASCO J-710 spectropolarimeter using 1 μM enzyme in 10 mM sodium phosphate buffer at pH 7.0 and the baseline obtained with buffer alone.[36] While collecting data, step resolution was kept at 0.2 nm per data point and scan speed was 50 nm/min. Sensitivity was kept at 20 millidegrees with a bandwidth of 1.0 nm. Each sample was scanned from 190 to 260 nm and an average of five accumulations was recorded using 0.05 cm path length cuvette. CD spectra of the composites ([GO] 0.15 mg/mL) were carried out in the same manner. The structure retention was calculated using ellipticity at 222 nm of native free GOx as the standard.

1.2.7 Enzymatic Activity Studies

The enzymatic activities of all the modified glucose oxidase samples was monitored by following a reported method.[37] GOx (1μM) was combined with guaiacol (10mM) and horseradish peroxidase (2 μM) in 10mM Na_2HPO_4 buffer. After equilibrating mixture, a solution of glucose (0.2mM) was added and oxidation of the substrate was monitored by recording the product absorbance at 470nm as a function of time. Kinetic traces were plotted using Kaleidagraph (V. 4.0) to determine initial rates and specific activities. Each experiment was repeated three times and data have been averaged.

1.2.8 Half-Lives of Enzymes

Enzyme stabilities were measured after storing them for extended periods of time, in the absence of its substrate, glucose. Activities of these samples were monitored as a function of storage time. Samples were stored at 40°C and activities have been measured at room temperature at intervals of 24 h until the activity decreased substantially. All activity studies were performed in 10mM Na_2HPO_4 buffer, pH 7.0 according to procedures described above. Specific activities vs. storage time were plotted (average of three measurements) and time taken to reduce the activity of the bioconjugate to half of its original activity (half-life) has been estimated from these data.

1.2.9 High Temperature Activity

Enzyme activity was monitored according to method described above after equilibrating GOx and GO/GOx samples in buffer at temperatures ranging from 25 - 95°C. Thermal inactivation kinetics were monitored by incubating native GOx, GOx (0), and GOx (66) in a water bath of denoted temperatures for 15 minutes. After incubation period, samples were immediately cooled to an internal temperature of 4 °C. Samples were then taken out of cold storage and loaded into activity cuvette with 10 mM phosphate buffer pH 7.0 held in a temperature controlled apparatus which was held at a constant temperature of 27 °C. Once solution internal temperature was equilibrated, activity of the heated samples was performed by adding HRP, guaiacol, and finally glucose to the stirring reaction mixture. Initial rates of incubated samples were then compared to unheated samples at 27 °C which was used as a control and percent activity retention was monitored.

1.3 Results

We tested the hypothesis that charge-charge repulsion contributes significantly to GOx instability (coulomb explosion). By using controlled covalent carboxyl modification techniques with amines to reduce the negative charge, we would theoretically be stabilizing the folded state, while its impact on the denatured state would be minimal. Our data shows that, when modifications are controlled under mild conditions, this approach produces modified GOx with increased isoelectric points (pI) and enhanced stabilities, while retaining secondary structure and activity to a significant extent.

1.3.1 Synthesis of Chemically Modified GOx

Covalent coupling of amines to the carboxyl functions was carried out under mild conditions by carbodiimide chemistry (**Scheme 1**). Coupling of GOx with ammonia, L-lysine, TETA, or TEPA under these specific conditions reduced the net negative charge, as indicated by agarose gel electrophoresis. Care was taken not to crosslink the enzymes by using excess amine and limiting the diimide concentration or the reaction time.

GOx is an ideal enzyme for this study due to the presence of 33 aspartic acid and 30 glutamic acid residues, which each carry a negatively charged carboxyl functional group at physiological pH. Bringing the pH of the reaction down to 5.0 was necessary for two reasons. First, due to the known isoelectric points of the amines used in the synthesis, a pH of 5.0 of the amines would allow for protonation of 75% of amine groups on TETA and 80% of amines on TEPA. Protonation of the amines is critical for reaction with activated carboxyl groups of the protein to create a covalent amide bond. Second, at pH 5.0 protonation of carboxyl groups of the protein is able to occur which is critical for the reaction with EDC. EDC was able to react with

the carboxyl group and create a better leaving group on the carboxyl, thereby activating it for reaction with the amines in solution.

1.3.2 Agarose Gel Electrophoresis

Reaction progress was monitored by agarose gel electrophoresis, where the protein sample is subjected to an external electric filed. The distance of migration in the gel is proportional to net charge on GOx, and the sign of charge is determined by the direction of migration. For example, native GOx is negatively charged at pH 7.0, and migrated toward the positive electrode (**Figure 1.1A**, lane 1). Since samples were applied at the center of the gel, the enzyme could migrate toward the anode or the cathode depending on its net charge at the pH of the buffer used for electrophoresis. Chemical conversion of a portion of the carboxyl groups of GOx to amides with L-Lysine, NH_4Cl, TETA, or TEPA resulted in GOx derivatives that migrated less toward the positive electrode and instead moved toward the negative electrode (lanes 2-8). Control lanes were run with a mixture of enzyme and the corresponding amines without EDC (**Figure 1.1B**), and the physical mixtures migrated just as GOx. The differences in migration of GOx and modified GOx, therefore, are concluded to be due to covalent modification of amine groups to the enzyme.

The gel obtained at pH 7.0 (**Figure 1.1A**) shows complete conversion of GOx to the modified enzyme and none of the lanes 2-6 indicated unreacted GOx. The attachment of TETA, which consists of four basic nitrogen groups, to GOx can introduce up to three positive charges per conjugation event, depending on the pH of the medium corresponding to the characteristic isoelectric point of the amine group on the TETA chain. Thus, chemical modification with

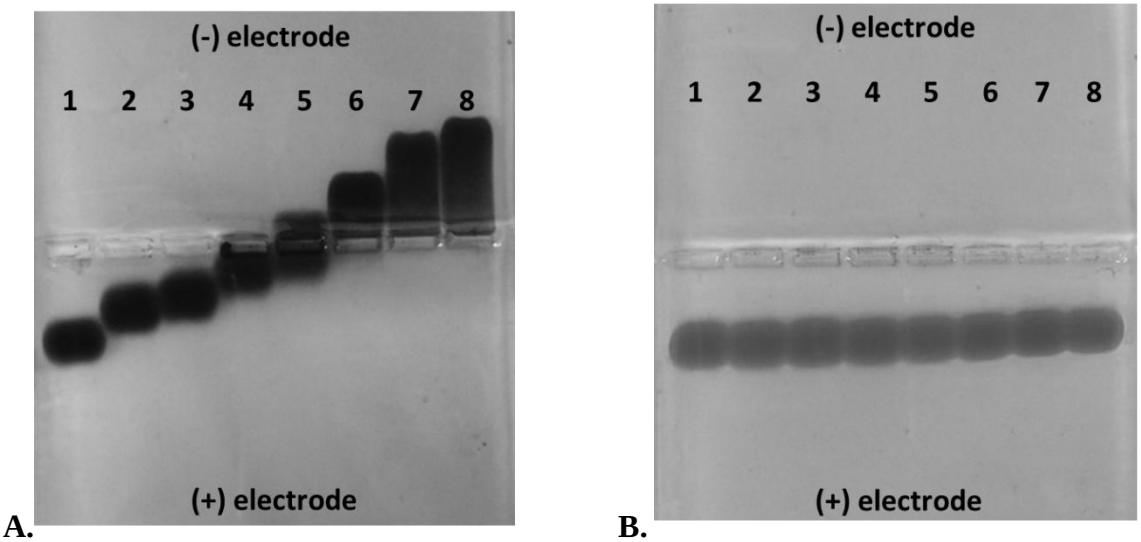

Figure 1.1. (**A**) 40mM Tris-Acetate agarose gels (pH 7.0) of GOx charge derivaties after EDC chemistry reaction to conjugate reactive amine group to surface carboxyl functional groups. (**B**) Physical mixture of GOx/amine derivatives without EDC present in reaction. Note that there is no migration difference in GOx when free amines are added without the activation of carboxyl groups via EDC chemistry. Lane numbers as they relate to specific samples are denoted in **Table 1.1**.

different types amines provided a simple method to systematically adjust enzyme net charge at a given pH.

1.3.3 SDS-PAGE

Chemical modification with multifunctional amines such as L-Lysine, NH_4Cl, TETA, or TEPA could crosslink two or more enzyme molecules due to the presence, in some modifiers, of multiple reactive amine sites. Also, the carboxyl groups on one enzyme molecule may couple with the amine groups on another and could result in modified enzyme dimers or higher aggregates involving the quaternary structure of GOx. Hence, the modified enzyme "charge ladder" was further characterized by SDS-PAGE to assess the extent of crosslinking, if any. According to **Figure 1.2.**, each gel contained the molecular weight markers in kD in the left-most well. Lane 1 contained unmodified GOx, and lanes 2-8 contained GOx charge modified derivatives, with charge of the enzyme increasing over the span of the wells. Modified GOx indicated predominantly the monomeric form of approximately 80kDa. Data showed negligible cross-linking of proteins at lower charges ranging from -65 to 0 (lanes 1-5) in the synthesis, however at higher charges, dimers of GOx were observed above 20% (lanes 6-8) with molecular weight of around 160 kDa. This data suggests that the when the synthesis occurs, higher concentration of polyamines that are present lead to the propensity to bind to sites on multiple protein targets, with less specificity than is observed at lower concentration of charged molecules. Physical mixtures of amine and protein displayed analogous lack of modification as was observed in agarose gel electrophoresis without EDC to create a suitable leaving group for the formation of an amide bond.

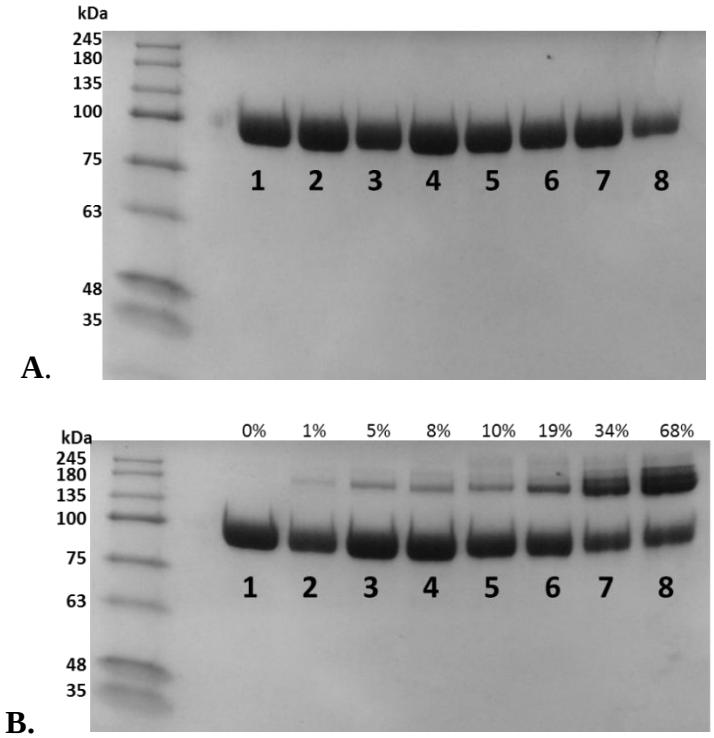

Figure 1.2. SDS-PAGE gels of physical mixture of GOx/amine (**A**) and GOx-amine after reaction with EDC (**B**). Lane marker numbers correspond to sample names as outlined in **Table 1.1**. Percent crosslinking in each reaction as determined by ImageJ software is noted above each well.

1.3.4 Structure Retention of Modified GOx

The CD spectra in the deep UV region (190-250 nm) of enzymes are characteristic of their secondary structure,[38] and significant decreases in the intensities of these CD bands or shifts in the peak positions would indicate corresponding loss of enzyme secondary structure. The CD spectra of charge-modified GOx derivatives are shown in **Figure 1.3A**, and display relatively similar CD spectrum to that of native GOx (black line). All measurements were recorded under the same conditions of concentration, path length, buffer and pH. Minor increases in the intensities of the 210 and 222 nm minima of the modified GOx indicated slightly tighter secondary structure than GOx. **Figure 1.3B** shows the percent structure retention of modified GOx samples when compared to that of unmodified GOx. The elipticity at 222nm of native GOx was taken to equate to 100% and the relative retention of structure for the charge-modified samples was compared to determine how much structure was lost after the synthesis. All samples displayed over 92% retention post-modification leading to the conclusion that no alpha helicies or beta sheets were disrupted during the chemical conjugation process. These data clearly show that careful, controlled chemical modification can be nearly benign. Therefore, we moved to the next phase of experiments to further evaluate the influence of these minor structural changes on the catalytic activities.

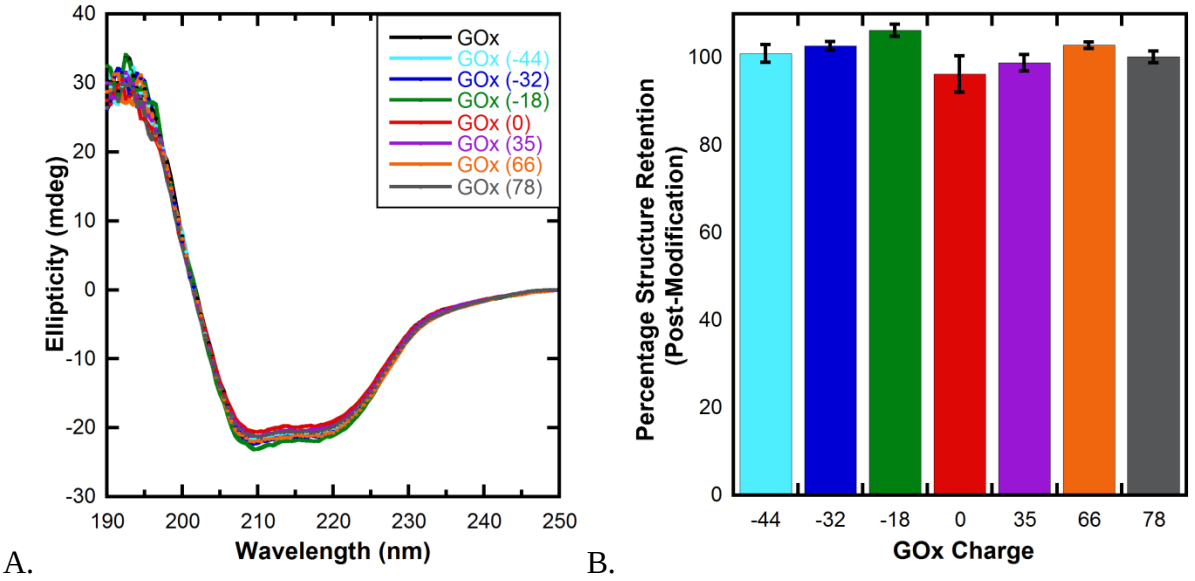

Figure 1.3. (A) Far UV CD spectra of glucose oxidase (black line), GOx (-44) (light blue line), GOx (-32) (blue line), GOx (-18) (green line), GOx (0) (red line), GOx (35) (purple line), GOx (66) (orange line), and GOx (78) (grey line) following chemical modification. (B) Secondary structure retention of GOx charge derivatives based on charge after modification when compared to structure of native GOx. Colors of the structure retention plot match the elipticity curves of CD spectra.

1.3.5 Enzymatic Activity of Modified GOx

Since the chemical modification has the potential to alter the active site residues directly or influence its catalytic role via allosteric effects, it is important to test the activities of the modified enzymes to assess the influence of chemical modification. The activities of natural and modified GOx samples are monitored using glucose as the substrate (**Scheme 1.2**). Addition of glucose to a mixture of GOx, HRP, and guaiacol in 10 mM phosphate buffer pH 7.0 resulted in rapid generation of the corresponding oxidation product, which has characteristic absorption maximum at 470 nm. Oxidation of guaiacol by hydrogen peroxide catalyzed by HRP was noted, where hydrogen peroxide has been produced by the catalytic oxidation of glucose by ambient oxygen, catalyzed by GOx.

The initial velocities of glucose oxidation catalyzed by GOx and its derivatives were extracted from the kinetic curves (**Figure 1.4A**). Percent activity retention was calculated relative to the specific activity of GOx and shown as the bar graph **(Figure 1.4B)**. Specific activity is essentially the same as that of GOx for charge adducts ranging from -44 to +35, all showing approximately 100% activity retention, with neutrally charged GOx displaying activity of about 115% compared to native. Activity showed some loss in the highest charged samples, with 94% and 85% in GOx (66) and GOx (78), respectively. Thus, chemically modified samples demonstrated that the modification process or alteration to the surface carboxyl groups did not alter the structure or function of the active site of the enzyme to a significant extent and may have in fact aided in the ability of GOx to process glucose.

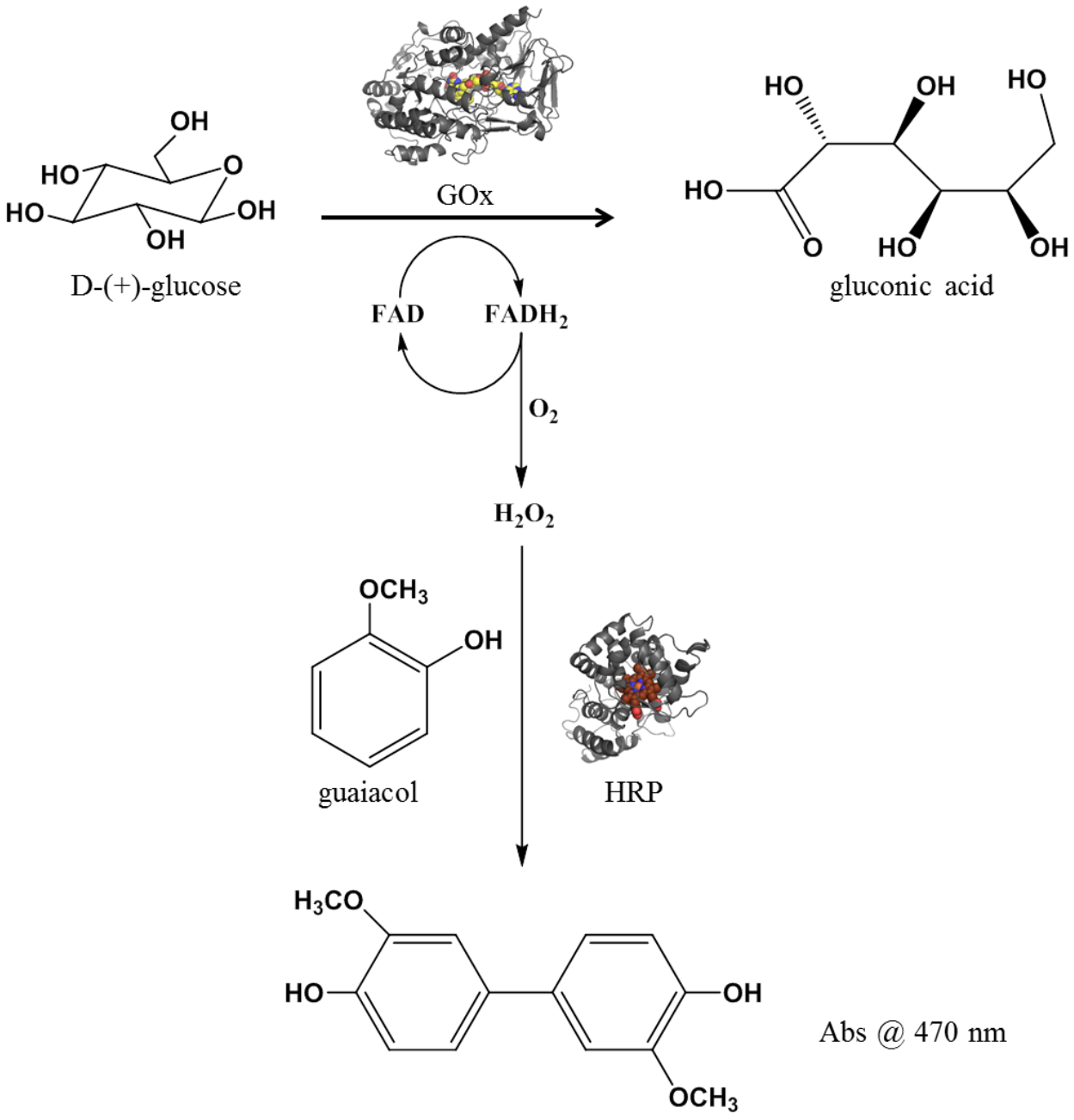

Scheme 1.2. Diagramed schematic of activity assay of modified glucose oxidase derivaties. GOx processes D-(+)-glucose to form gluconic acid and hydrogen peroxide (H_2O_2). Presence of horseradish peroxidase (HRP) utilizes available H_2O_2 and guaiacol to form oxidation product whose generation can be monitored spectrally at 470 nm. Each mole of glucose processed by GOx leads to equivalent formation of oxidation product.

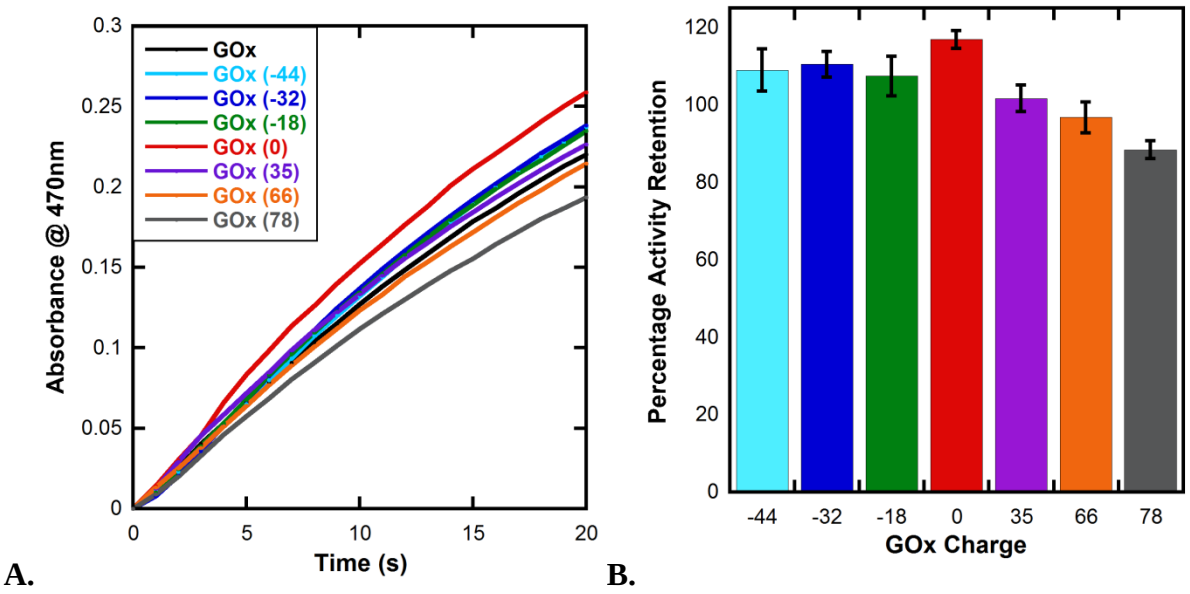

Figure 1.4. (A) Comparison of activities of 1 μM GOx (black line) and charge modified GOx samples. (B) Percentage activity retention of modified GOx derivatives based on charge relative to native GOx. Color scheme of samples matches that described in **Figure 1.3**.

1.3.6 Storage Stability of Modified GOx

Due to the retention in both structure and activity, we used these samples to test the hypothesis that enzyme solution stability is directly related to enzyme charge using storage half-lives under the same conditions of pH, buffer and ionic strength. Modified enzyme samples were stored at 40˚C in the absence of substrate, and aliquots were withdrawn periodically to measure their enzymatic activities as a function of storage time.

According to the above hypothesis, charge reduction at enzyme-water interface should increase enzyme half-life, and we examined activities of GOx-derivatives after storing them for extended periods of time. Specific activities obtained from these data are plotted as a function of storage time (**Figure 1.5**), and time required to reduce the initial activity of the modified enzyme by half (half-life) has been estimated from these plots (**Table 1.2**). Enzyme activities have been monitored for nearly 25 days to obtain accurate measurements of all half-lives, as some samples indicated higher stability.

The half-lives of GOx derivatives increased up to 10-fold higher than unmodified GOx, from 0.55 days for GOx to 5.66 days in GOx (0). A trend is noted of increasing half-life in charge modified samples with maximum stability at net neutral charge at pH 7.0.

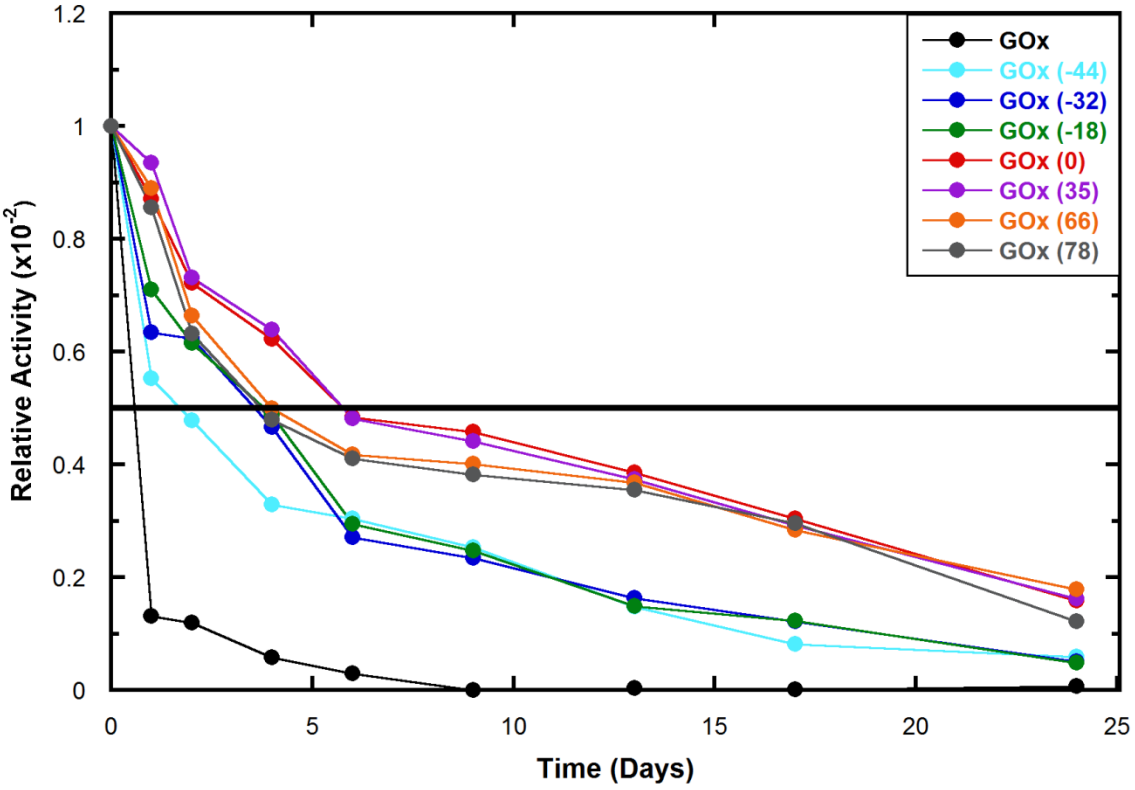

Figure 1.5. Plot of relative activities of 4 μM charge-modified GOx samples stored at 40 °C relative to initial reading of activity for GOx derivative at respective charge as a function of storage time. Decline of activity at 40 °C followed first order kinetics for all samples and were stored at elevated temperature to measure half-life in laboratory time frame. Activity studies conducted after equilibrating aliquots to room temperature (27 °C) so maintain uniform temperature of assay throughout.

Table 1.2. Half-lives of chemically modified GOx derivatives at 40°C. Enzyme (4 μM) was kept in 10mM Na_2HPO_4 buffer pH 7.0 and stored in water bath in the absence of substrate. Aliquots of each sample were removed at measurement intervals and allowed to cool to room temperature before measuring activity.

GOx Bioconjugate Charge	**Half-life in Days**	**Percent Increase in Half-Life**
-67 (native)	0.55 ± 0.21	-----
-44	1.69 ± 0.46	307%
-32	3.52 ± 0.17	640%
-18	3.75 ± 0.15	681%
0	5.66 ± 0.22	1030%
35	5.45 ± 0.31	990%
66	3.96 ± 0.28	720%
78	3.64 ± 0.18	662%

To investigate if the net charge reduction correlated with their half-lives, we plotted half-lives as a function of their respective charge values **(Figure 1.6)**. The data clearly show a strong trend with a steep increase in half-lives with increased charge before experiencing a decrease in half-life when the charge exceeds 35. The lowest stability was noted with GOx, which has a pI of 4 and highest overall negative charge. The highest half-life was observed with GOx (0) which is net neutral at pH 7.0. The GOx (35) sample half-life was also within range of GOx (0), which displays an optimum charge range of GOx as it pertains to its solution stability and storage. GOx (66) which has approximately the opposite net charge of unmodified GOx displayed greater than 720% increase in storage stability when compared to its negatively charged counterpart. Chemical modification therefore may have other stabilizing effects on the enzyme other than relieving coulombic stress of the system. Such increased solution stability led us to test the stability of the modified proteins under further thermally unfavorable conditions.

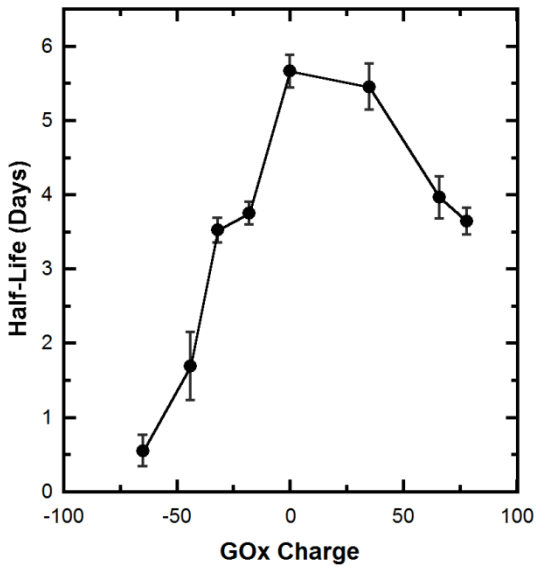

Figure 1.6. Plot of half-live vs. enzyme net charge of native GOx and GOx charged derivatives. Stability increases with increased charge with a maximum half-life at net neutral charge at pH 7.0. Further increase in charge leads to destabilization of the enzyme and likewise decrease in overall half-life.

1.3.7 High Temperature Activity of Modified GOx Samples

All charge-modified GOx samples displayed increased half-life and thereby demonstrated greater solution stability when compared with native GOx. Encouraged by the increased kinetic stability, we chose to investigate if the thermal stability of GOx was affected by the reduction of net charge and the chemical modification process as a whole. To accomplish this, GOx (0), which displayed the greatest stability at 40°C over time, was subjected to higher thermal stress. Activity studies were performed as a means of quick analysis of the sustained enzyme functionality in increasing temperatures (**Figure 1.7**).

In order to ensure data would reflect true thermal stability of the protein rather than reinforcing the kinetic stability principles that were shown in the half-life studies, the enzymatic activity was not only conducted at the desired temperature, but the protein sample being tested was subjected to the heating conditions for up to 20 min before substrate was added. This equilibration time meant the protein would be within the heated environment for a substantial amount of time to correctly reflect whether or not structure was retained to the point where activity were still possible.

Data show that the chemical modification process led to enhanced thermal activity stability over unmodified GOx. GOx (0) retained 30% of its initial activity at 65°C whereas native GOx displayed zero activity at 65°C. It should also be noted that while GOx showed only 81% activity at 55°C, GOx (0) activity was nearly 100% of the original. The process of reducing the net charge of the GOx protein to a neutral state therefore has shown to stabilize the enzymes kinetic function and increase resistance to thermal denaturation.

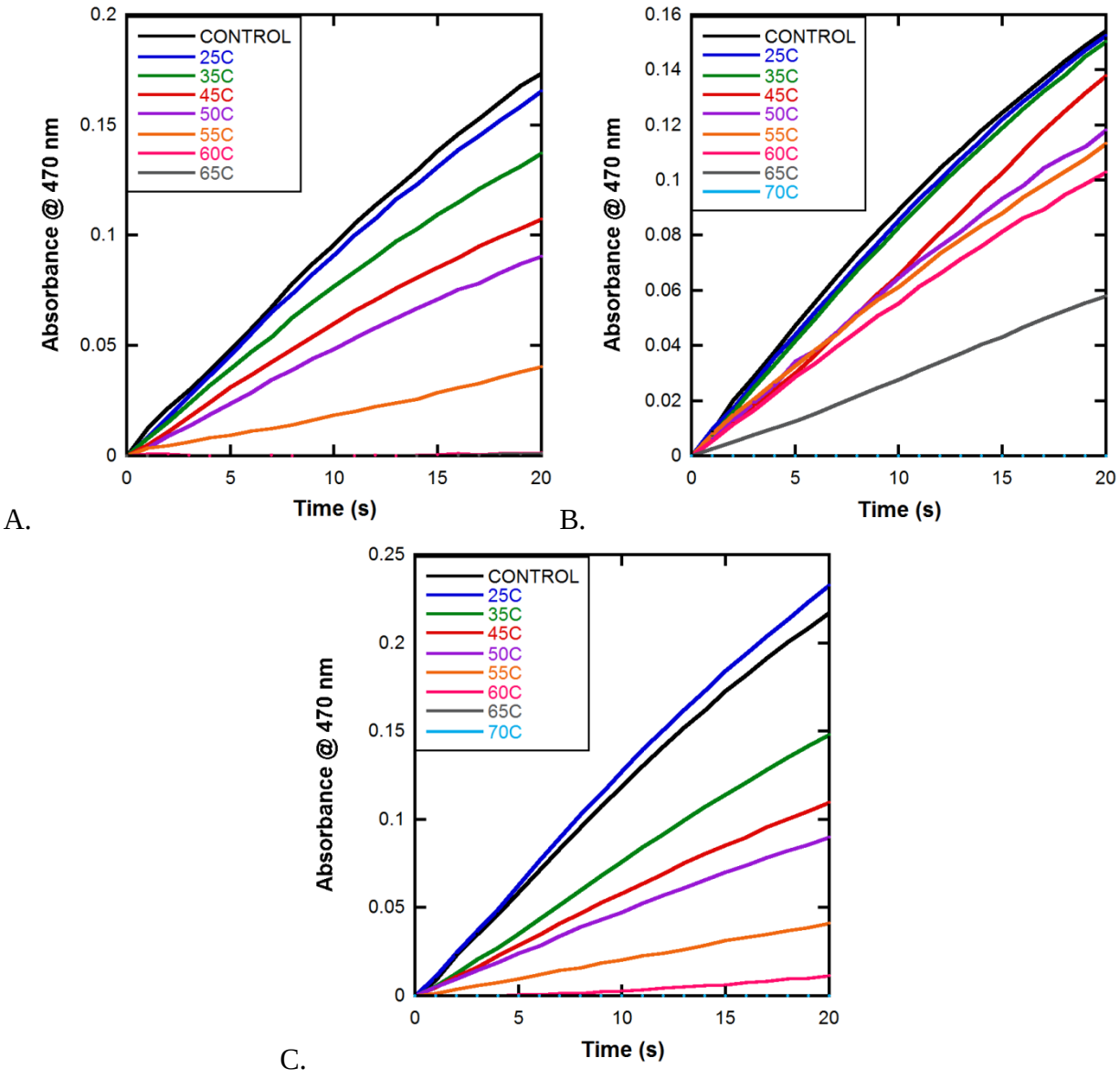

Figure 1.7. Temperature dependence activity data of native GOx (A) and GOx (0) (B) and GOx (66) (C) over increasing temperatures from 25 - 70°C. GOx (0) shows retention of activity after equilibration at 65°C for 15 min whereas the native GOx enzyme is rendered inactive by the increased temperature of the environment at temperatures exceeding 55 °C. GOx (66) displays characteristics similar to that of native GOx, which has an overall charge of -65 at pH 7.0, meaning temperature effects appear to be characteristic of charge of system rather than a result of PCM process.

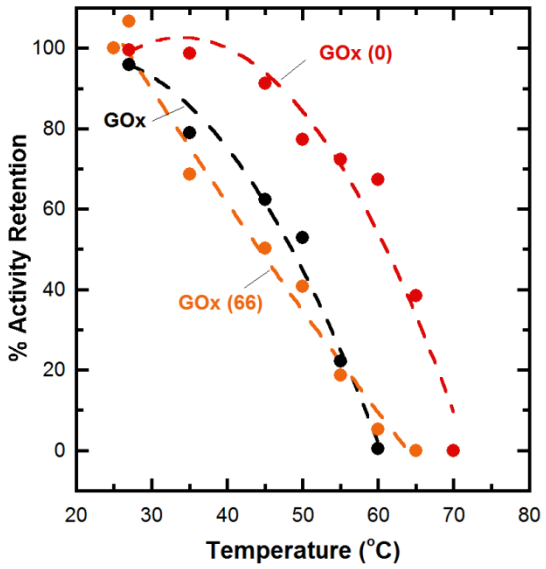

Figure 1.8. Thermal inactivation of GOx based on activity retention of native and modified GOx derivaties. Samples were stored at above displayed temperatures for 15 minutes, then immediately cooled to 4 °C. After cooling period, samples were equilibrated to room temperature in order to measure activity at constant temperature.

1.4 Discussion

Chemical modification of enzymes can provide a simple method to modify their surface residues, and thereby alter the net charge of the protein. This has the potential to affect the enzyme-water interface, reduce surface tension of the enzyme complex, and lead to enhanced conformational stability of the active enzyme structure. Though a clearer understanding of the basis for these changes at the molecular level is needed, harnessing this method of effective charge manipulation can be a breakthrough in obtaining control over types and extents of physical and chemical modifications required for a desired outcome of nanoscale reactions. The main focus in the area of chemical modification of enzymes has been largely limited to direct applications of the modified enzymes, rather than toward understanding their stability or the underlying causes for the altered behavior. To address these issues, the current study investigates the systematic alteration of enzyme surface residues in a model system to examine the influence of net charge at the enzyme-water interface on their stabilities.

Clearly, the chemical modification altered enzyme charge values over a range of -65 to +78, due to the removal the negative charge of carboxyl groups by converting them to the amide form of the corresponding amine used in the synthesis. L-Lysine reacting with the system would lead to charge neutralization of the negatively charged carboxyl group at physiological pH that was subject to modification, due to the reaction with the amine of the R-group and the ionization of both amine and carboxyl terminal groups. NH_3^+ would not only negate the negative charge of the reacting carboxyl, but would also carry a positive charge due to the protonation of the amine, leading to the replacement of a -1 charge with a +1 charge in the same region. The presence of additional basic nitrogens present in TETA and TEPA will remain protonated at neutral pH, further reducing the negative charge to a greater extent with the same amount of modified

groups. Therefore, the increase in charge depended on the amine used as well as the extent of modification on GOx.

Chemical modifications carried out here are mild and did not cause any significant structural changes as indicated by the CD data. If the chemical modification altered key residues at the active sites of GO and distorted their structure substantially, activities of the modified GOx would have decreased substantially. Consistent with this claim, activity studies show that modified GOx show 100% - 85% retention of activities as displayed in **Figure 1.3**. Maintaining this level of activity shows that both the type and extent of modification used in this process has not hindered the ability of the enzyme to function properly, and could therefore still be used as a viable alternative to native GOx in reactions. This is important because chemical modification of key residues at the active site of GOx or residues at the entry port of the active site could have deactivated the enzyme completely, but in fact have had a much more benign effect.

To determine how robust the modified enzyme samples were we performed tests to find the temperature of inactivation as it pertains to the kinetic abilities of the enzyme. Native enzyme was shown to be rendered completely inactive in temperatures in excess of 55 °C, however the chemical modification process that led to neutral charged enzyme derivatives displayed activity up to 65 °C. Further extent of chemical modification did not lead to greater resistance in thermal denaturation as displayed in **Figure 1.8.** where GOx (66) in fact displayed thermal characteristics similar to that of the native GOx rather than the GOx (0) sample. At highly positive or negative charges, a distinct pattern is shown as it relates to the stability of the protein under thermally unfavorable conditions. Lowering the net charge to the lowest point of a theoretical energy well will result in an enzyme with the greatest amount of stability when it comes to unfavorable thermal environments.

The most significant feature of chemically modified GOx was the substantial improvement of solution storage stability. When samples were stored in the absence of the substrate at 40 ˚C, in pH 7.0 phosphate buffer, the stabilities improved rapidly corresponding to increased charge. **Figure 1.6** shows that the highest stability was observed when the net charge of the enzyme was 0, and decreases regardless of if charge of the enzyme is increased or decreased. The storage stability of the protein therefore appears to have maximized when benign modifications to the protein surface was carried out to neutralize the charge in solution. It has been reported that presence of additives, such as lysozyme or sodium chloride, have the potential to increase the ability of glucose oxidase to resist thermal denaturation.

Though these additives have no particular impact on activity of the enzyme, presence of lysozyme, a protein with a pI upwards of 11.35 at physiological pH, can reduce the net charge of the solution and relieve solution strain of highly negatively charged GOx. A similar reduction of net charge can be achieved by covalent modification of the GOx as we have displayed here. The maximum amount of stabilization therefore would be thought to occur when a concentration of lysozyme is added that would render the net charge of the solution to zero.

Addition of sodium chloride or other high/medium charge density anions (phosphates, sulfates, chlorides, etc.) will also yield higher stabilized protein samples due to the lowering of bulk water concentration at high anion concentrations.[39] As the protein begins to unfold, the hydrophobic molecules exposed to the solvent will recruit water molecules to stabilize the additional free energy being introduced to the system. If there are too many anions competing with water in solution for the hydrolysis of the unraveling protein, the free energy needed to hydrate the exposed hydrophobic core of the protein rises substantially, and therefore the protein will remain folded due to lack of energy in the system.

The increased stability is theorized to come from a variety of contributing factors. One explanation is that the introduction of polar charges on the surface of the protein increases solubility of the protein by promoting new polar interactions at the enzyme-water interface. The increased polar contacts with the water molecules will lower the propensity of the enzyme to aggregate due to exposed non-polar residues, leading to increased life-time in a native like state and thereby prolonging activity. Another explanation is that the reaction of newly covalently attached amine groups with carboxyls of GOx lowers the charge-charge repulsion of the high amount of negative charged surface residues. Lowering repulsive tension by placing a favorable positive charge near an area of dense negative charge would relieve coulombic strain on GOx. These islands of high negative charge density have the potential to stress and destabilize large regions of the protein and lead increased probability of aggregation.

It has also been shown that by using site-specific mutagenesis, new intramolecular hydrogen bonds and salt bridges could be formed on the surface of a protein to help prevent unfolding upon subjection to heat.[40, 41] Newly added positive charges on the surface of the protein in close proximity to a negatively charged residue could have the potential to form new, induced salt bridges and H-bonds that stabilize protein conformation, which was shown by CD data in **Figure 1.3** to have maintained a catalytically active conformation. A higher number of salt bridges in the protein will lead to an increase in the energy barrier of unfolding,[42] allowing for proteins to remain in the active folded state for a longer period of time.

Additional insight into the stability may be gained by examining the number of carboxylic groups on the enzyme that are available for chemical modification. Glucose oxidase has 126 aspartic and glutamic acid residues which provide ample opportunities for increasing the stability by charge neutralization via chemical modification.

1.5 Conclusions

Although chemical modification of enzymes has been known and practiced for some time, there has been no systematic evaluation of the influence of the chemical modification on key properties of the modified enzymes, nor is there a systematic study of how altering side chains would influence the thermal or storage stabilities. A general strategy is described here to systematically control the charge and isoelectric point of GOx by chemical conjugation without compromising its structure or activity. We tested the hypothesis reducing coulombic strain and charge- charge repulsion via chemical modification would be related to enhanced solution stability of GOx.

A small set of amines with increasing numbers of positive charges per chain is used successfully. Modification with this small set of ligands show that key properties of the enzyme are essentially independent of the amine used but related more to how the charge and electrostatics of the target are changed. The enzyme charge has been controlled systematically by increasing the number of basic groups conjugated to the ligand. This resulted in the production of strongly positively charged enzymes at physiological pH without compromising their secondary structure, stabilities or activities.

We conclude that chemical modification of proteins, when done carefully, is a viable method to modulate the enzyme-water interface and electrostatic composition without considerable loss in their structure, as evidenced by the CD data. Minor changes in the CD of some samples can be anticipated due to a decrease in repulsion or change in the surface characteristics of the enzyme but these changes are not substantial. The chemical modification also did not adversely influence GOx activities.

One interesting conclusion is that GOx stability has been improved by simple chemical modification and the extent of stabilization correlated with net charge. For example, at neutral pH the net charge on GOx is strongly negative and appropriate chemical modification with TETA produced a near-neutrally charged enzyme. Since carboxyl-carboxyl repulsion energy ($\Delta G_{repulsion}$) is expected to increase with increasing numbers of carboxyl groups, enzymes with the largest negative charge (lowest pI), may provide the greatest opportunities for increasing their stability. This hypothesis will be tested in future studies, and chemical modification, therefore, may provide a powerful tool to manipulate enzyme-water interface which plays an important role in a number of enzyme physical and biochemical properties.

Chapter 2

Protein Chemical Modification as a Powerful Tool to Stabilize Protein-Graphene Oxide Bio-hybrids

2.1 Introduction

Here, chemical modification approaches are used to systematically enhance the kinetic and thermodynamic stabilities of enzyme/graphene oxide bio-hybrids with stabilities lasting over months, even at 40 ˚C. The enzyme-graphene interface (EGI) which plays a key role in these advanced biocatalysts has been optimized via chemical modification of the enzyme functional groups in the current studies, and EGI is being intensely investigated for a myriad of applications in biosensors,[43, 44, 45] biocatalysis,[46 47, 48, 49] biofuel cells,[50] biomedicine[51, 52, 53] and other applications. Graphene oxide (GO), the water dispersible derivative of graphene, in principle, is an ideal adsorbent for biomolecules because of its high surface area (7.05×10^{22} $Å^2/g$),[46 ,54] excellent thermal/electrical properties and low cost. [55,56] Bio-hybrids consisting of biological components embedded in graphene bring together the desirable properties of the biological component and the exciting physical/chemical attributes of graphene to produce advanced materials for practical applications.

Thermodynamic stability of enzymes at the EGI was improved by decreasing the number of microstates of the denatured state of the protein or by simply stabilizing the native state.[57] This was partly achieved, for example, by constraining the protein between the two dimensional galleries of α-Zirconium (IV)-Phosphate nanoplates.[58] On the other hand, kinetic stability of bio-hybrids is also important but has not received substantial attention.[59] When continuous performance of a biomolecule is required for a prolonged period such as in a bioreactor or biofuel cell, kinetic stability is of significant importance just as its thermodynamic stability. The fundamental question is, how to control the kinetics of protein denaturation and inactivation and extend the usable lifetime of enzymes in advanced bio-hybrids?

Protein kinetic stability can be improved and its high half-life ($t_{1/2}$) increased by raising the activation barrier leading to the unfolding pathway. Site-specific mutational studies have shown that protein longevity can be improved by manipulation of amino acid sequences.[60] However, approaches independent of the protein engineering are sparse and properly designed bio-nano interactions can enhance protein kinetic stability. In order to do so it is critical to understand the driving force leading to a favorable interaction at the Bio-nano interface. One hypothesis is that the electrostatic interactions between the bound enzyme and the solid surface need to be matched for highest stability of the native state of the bound enzyme (lowest free energy state), and this optimum situation will also result in considerable destabilization of the corresponding denatured state. These conditions might also raise the activation energy barrier for unfolding of the bound protein and increase the kinetic stability of the bound enzyme. Thus, we are testing the hypothesis that charge-matching between the bound enzyme and the binding surface is a key property to control stability of the bound enzyme.

The early development of EGI predicts the role of favorable electrostatic and hydrophobic interactions leading to stable protein/GO conjugates. Here, we investigate utilizing charge control of the protein surface, rather than to the surface of GO, to enhance affinity of protein to GO and stabilize BGI. Controlled, benign modifications described in this report can provide a favorable mechanism to assemble catalytically viable proteins with the functionally versatile GO can then be tuned for specific targets and applications

Glucose oxidase (GOx) is chosen as a model protein for the above studies. GOx is a homodimeric glycoprotein that utilizes molecular oxygen to oxidize β-D-glucose to gluconic acid under ambient conditions. GOx has a net charge of -65 at pH 7 and carries 126 carboxyl groups which can be modified into their corresponding chemical derivatives (**Scheme 1, top**).

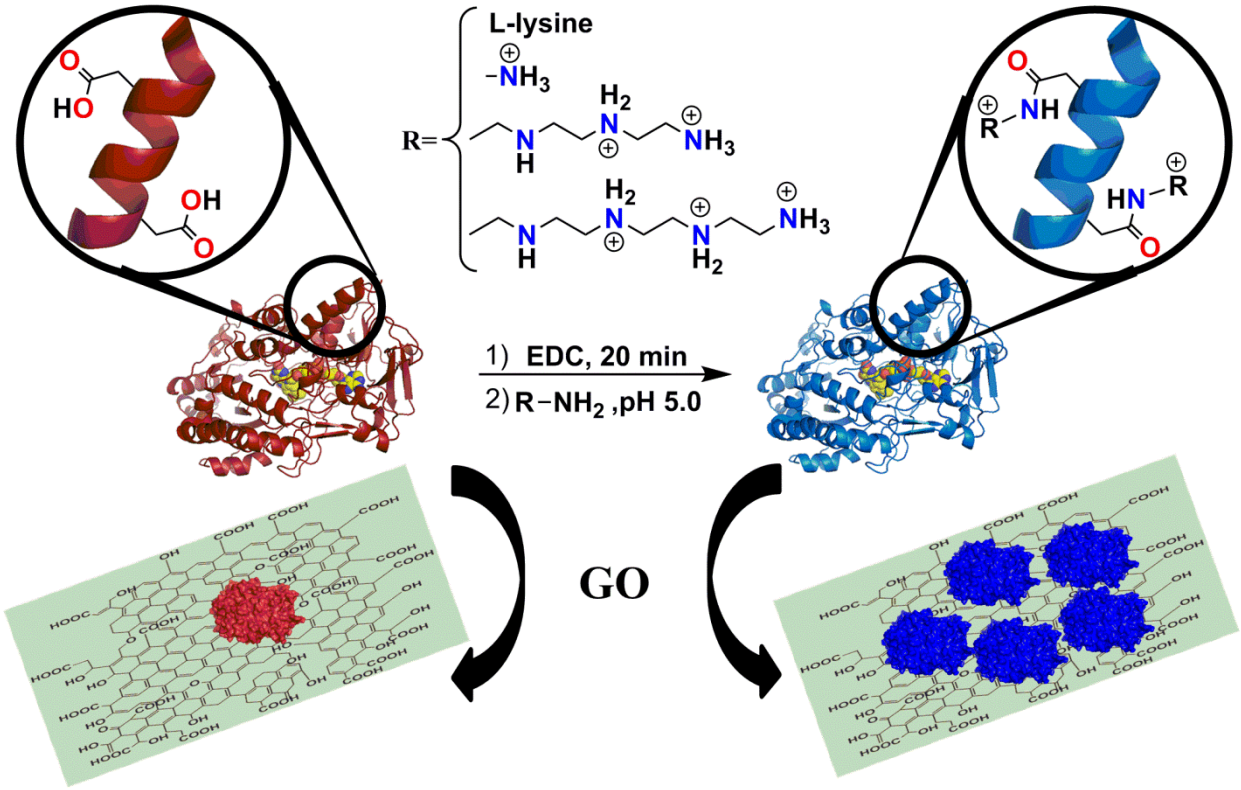

Scheme 2.1. Chemical modification of native glucose oxidase (red) to create positively charged cationized GOx (blue) via non-covalent binding of various amine R-groups in non-specific fashion. Binding to graphene oxide (GO) sheets is enhanced after protein surface alterations due to addition of positive charges reacting favorably with negatively charged carboxyl groups on the GO surface.

Thus, GOx has excellent potential for a systematic chemical modification of its structure and we evaluate how the structure changes are related to the changes in its physical, chemical and biological properties.

In the native state, the strong negative charge of GOx can destabilize the structure due to unfavorable charge-charge interactions between the residues[61,62] and the intrinsic affinity of GOx to the negatively charged GO is also very poor.[49] However, conversion of the COOH groups of GOx into the corresponding amide functions, for example, can alleviate these unfavorable repulsions and therefore expected to improve protein stability (**Scheme 1**). Reduction of the net negative charge of GOx by chemical modification is also expected to enhance its affinity for the negatively charged GO, and thus protein chemical modification (PCM) provides an excellent handle to optimize the EGI for control of bound enzyme stability. Data presented here show that optimally charged GOx *via* PCM enhances its binding to GO, maximizes bound enzyme kinetic stability and resistance to deactivation has been greatly enhanced even at 40 ˚C. These details are presented here.

2.2 Experimental

2.2.1 Chemicals and Materials

Glucose oxidase (GOx) from *Aspergillus niger*, L-Lysine, Ammonium Chloride (NH_4Cl), Triethylenetetramine (TETA), Tetraethylenepentamine (TEPA), D-(+)- glucose, Guaiacol, Graphite, and sodium phosphate dibasic (Na_2HPO_4) were purchased from Sigma-Aldrich Co. (St. Louis, MO). Horseradish Root Peroxidase (HRP) was purchased from Calzyme Laboratories, Inc. (San Luis Obispo, CA). N-(3-dimethlaminopropyl)-N-ethylcarbodiimide (EDC) was purchased from TCI America (Portland, OR).

2.2.2 Protein-Polymer Conjugate Synthesis

Enzyme samples were modified by reacting the carboxyl functional groups of enzymes with appropriate amines, by adopting reported procedures. As an example, GOx (3 mg/ml) in deionized water (DI) was stirred with TETA stock, pH adjusted 5.5, for 30 minutes followed by the addition of EDC. The mixture was stirred for four hours at room temperature and unreacted EDC, TETA, and other byproducts were removed by dialysis against 10mM phosphate buffer (Na_2HPO_4) using 50kDa MWCO dialysis membrane from Spectrum Laboratories, Inc. (Rancho Dominguez, CA). This approach was also used for enzyme modification with other amines. The degree of modification was carefully controlled by adjusting EDC and amine concentration, pH of the reaction mixture, enzyme concentration and the reaction time until all GOx has been reacted. **Table 2.1** contains reaction conditions of note needed for successful modification of GOx.

Table 2.1. Reaction conditions used for the bioconjugate preparation. Optimized concentrations of amines (mM) and enzymes (3 mg/ml) (pH 4.5- 5.2) in Na_2HPO_4 (10 mM), at 25 ^{0}C. Reaction stirred for 4 hours after addition of EDC.

Bioconjugate Sample	**Amine Concentration-Synthesis**	**Amine/ Reaction pH**	**Lane Number (Figures S1 & S2)**
Glucose Oxidase (GOx)	---	5.0	1
GOx (-44)	5 mM TEPA	5.0	2
GOx (-32)	50 mM L-lysine	4.5	3
GOx (-18)	100 mM NH_4Cl	5.0	4
GOx (0)	10 mM TETA	5.2	5
GOx (35)	20 mM TETA	5.2	6
GOx (66)	50 mM TETA	5.2	7
GOx (78)	70 mM TEPA	5.2	8

2.2.3 Graphene Oxide Synthesis

GO was synthesized by following modified Hummer's method[63] reported elsewhere.

2.2.4 Modified Glucose Oxidase-Graphene Oxide Binding Studies

After synthesis of modified GOx derivatives, binding studies were performed by addition of GOx in varying concentrations ranging from 1- 10 μM protein to 0.15 mg/mL GO to assess the binding based on charge. After allowing samples to equilibrate under gentle stirring conditions for 90 minutes, samples were centrifuged at 12,000 rpm for 20 minutes to form a pellet of GO and corresponding GOx bound to the surface. After centrifugation, absorbance at 280 nm of the supernatant was taken and concentration of unbound protein was determined from the known loading protein concentration. From this data, a binding plot was able to be constructed based on the surface charge of the GOx samples added.

2.2.5 Zeta Potential Studies

Laser Doppler velocimetry method in a Zeta Potential Analyzer (ZetaPLus, SR-516 type electrode, Brookhaven, Holtsville, NY) was used to measure the zeta potential of GO-GOX suspensions. Sample suspensions in 10 mM sodium phosphate buffer at pH 7.0 containing GO (0.65 mg/mL) were stirred for 4 hours with GOX solutions (14 μM) at room temperature prior to the measurements. Electrophoretic mobility of the samples (1.6 mL) was measure in a polystyrene cuvette (4 mL) and zeta potential values in mV were calculated using Smoluchowski fit provided by the manufacturer.

2.2.6 Transmission Electron Microscopy (TEM) Analysis

A suspension of GO/GOx-TETA (0) was placed on a carbon coated Cu-grid and stained using uranyl acetate and allowed to dry at room temperature overnight.

2.2.7 Circular Dichroism (CD) Studies

The CD spectra were recorded on a JASCO J-710 spectropolarimeter using 1 μM enzyme dissolved in 10 mM sodium phosphate buffer at pH 7.0 and the baseline obtained with buffer alone. While collecting data, step resolution was kept at 0.2 nm per data point and scan speed was 50 nm/min. Sensitivity was kept at 20 millidegrees with a bandwidth of 1.0 nm. Each sample was scanned from 190 to 260 nm and an average of five accumulations was recorded using 0.05 cm path length cuvette. CD spectra of the composites ([GO] 0.15 mg/mL) were carried out in the same manner. The structure retention was calculated using ellipticity at 222 nm of native free GOx as the standard.

2.2.8 Enzymatic Activity Studies

The enzymatic activities of all the modified glucose oxidase samples by following a reported method. GOx (1μM) was combined with guaiacol (10mM) and horseradish peroxidase (2 μM) in 10mM phosphate buffer. After equilibrating mixture, a solution of glucose (0.2mM) was added and oxidation of the substrate was monitored by recording the product absorbance at 470nm as a function of time. Kinetic traces were plotted using Kaleidagraph (V. 4.0) to determine initial rates and specific activities. Each experiment was repeated three times and data have been averaged.

2.2.9 Heat-Stress Half-Lives of Enzymes

Enzyme stabilities were measured after storing modified GOx and GOx-GO conjugates for extended periods of time, in the absence of glucose to compare thermal stability. Activities of enzymes were monitored as a function of storage time. Samples were stored at 40°C and activities have been measured at room temperature at intervals of 24 h until the activity decreased substantially. All activity studies were performed in phosphate buffer (Na_2HPO_4 (10mM), pH 7.0), according to procedures described above. Specific activities vs. storage time were plotted (average of three measurements) and time taken to reduce the activity of the bioconjugate to half of its original activity (half-life) has been estimated from these data.

2.2.10 Temperature Stability Studies

Enzyme activity was monitored according to method described above after equilibrating GOx and GO/GOx derivaties in water bath at desired temperatures for 15 minutes. Samples were incubated and monitored until internal solution temperature reached desired level then allowed to remain at temperature for 15 minutes before being removed from heat and immediately cooled to an internal solution temperature of 4°C. After cooling was completed, samples were re-equilibrated to room temperature (27°C) before measuring activity to ensure all samples were of equal temperature during experimental period.

After initial heating period, guaiacol and HRP were added and finally glucose was introduced to mixture and activity was monitored. Each experiment was repeated three times for accuracy and data for each trial were averaged.

2.2.11 Chemical Stability Studies

Resistance to denaturation under increasing Guanidine hydrochloride (Sigma-Aldrich) concentration or enzyme and enzyme-GO samples was measured. 1 μM GO-GOx conjugates or GOx controls were prepared and added to GdCl ranging from 0-6 M denaturant and then allowed to equilibrate for 1 hour at room temperature. Circular dichroism spectra was collected and ellipticity of samples at 222nm was measured to determine loss of secondary structure in the α-helical regions of GO corresponding to unfolding of the protein. Ratio of native structure to denatured protein was then calculated based on change in ellipticity to monitor the point at which 50% of the sample was denatured.

2.2.12 Activation Energy Calculations of ΔG* and E_a

The thermal and kinetic stability of GOx in the presence and absence of graphene oxide was determined by the inactivation rate constant (k_r) which was determined by the percent activity retention of the enzyme as a function of time. The values for free energy of inactivation (**ΔG***) of different modified samples was obtained from equation (1):

$$\Delta G^* = -\mathrm{RTln}(^{k_r h}/_{k\mathrm{T}})$$

Where *h* is the Planck constant, *k* is the Boltzmann constant, and T is the temperature in Kelvin. Activation energy was determined using equation (2):

$$\frac{k_r}{k_r'} = e^{(^{Ea'}/_{Ea})}$$

where k_r` and $E_a$` are the inactivation rate constant and activation energy of the modified samples, respectively. k_r` was able to be experimentally calculated based on the half-life of each individual GO/GOx derivative sample tested, which would lead to the calculation of $E_a$`.

2.3 Results

Stability studies of GO/GOx conjugates were studied from both a thermodynamic and kinetic perspective here. The design principles for functional graphene biomaterials were analyzed by systematic charge modulation of the protein surface. Our data suggests that charge control at BGI is necessary for optimum adsorption characteristics as well as for kinetic stability of proteins.

2.3.1 Synthesis of Chemically Modified GOx

The COOH groups of aspartic and glutamic acid side chains of GOx are modified systematically by covalent attachment of polyamines, as shown in **Scheme 1.1**, using EDC chemistry. Coupling with L-lysine, ammonia, triethylenetetramine (TETA), and tetraethylenepentamine (TEPA) resulted in a decrease in the negative charge of the protein and progress of the reaction has been monitored by agarose gel electrophoresis (**Figure 1.1**). PCM resulted in GOx derivatives, essentially a charge ladder, and the gel mobility has been used to estimate the net charge on the modified protein. Based on the charge obtained from modified GOx migration on the agarose gel, samples will be referred to in terms of their modified charge as outlined in **Table 2.1** such as GOx (-44), GOx (-32), and so on. PCM derivatives were previously characterized by SDS-PAGE, circular dichroism, and activity assays to determine detrimental effects after chemical modification process. Important information such as changes in charge, percentage dimerization, percentage structure retention, and percentage of enzymatic activity retained are also outlined in **Table 2.1**.

Table 2.2. PCM of GOx resulted in a charge ladder with the following properties. Structure and enzymatic activity of native GOx was taken to be 100% when comparing chemically modified samples.

Bioconjugate Sample	**Bioconjugate Reference #**	**Bioconjugate Charge at pH 7.0**	**Dimerization (%)**	**Structure retention (%)**	**Enzymatic activity retention (%)**
Native GOx	1	-65	---	---	---
GOx- TEPA (5)	2	-44	1	101.0	107.3
GOx- Lysine	3	-32	5	102.7	109.6
GOx- NH_4Cl	4	-18	8	106.3	105.2
GOx- TETA (10)	5	0	10	96.23	118.3
GOx- TETA (20)	6	35	19	98.82	101.1
GOx- TETA (50)	7	66	34	102.9	94.7
GOx- TEPA (70)	8	78	68	100.2	88.5

2.3.2 Preparation of GO/GOx Bio-hybrids

The hypothesis that PCM can be used as a powerful tool to modulate the EGI and enhance favorable interactions with GO are tested in equilibrium binding studies as well as Zeta potential measurements. GOx (4 μM) and its derivatives were equilibrated with exfoliated GO (0.15 mg/mL) for 1 hour, centrifuged to remove the bound protein, and the amount of unbound protein has been determined by examining the absorbencies of the corresponding supernatants. Binding isotherms of protein to GO are shown in **Figure 2.1**.

PCM improved the loading as a function of increased charge, initially, reached a maximum and then began to decrease at high charges of +66 and +78 (**Figure 2.1A**). When GOx was modified with NH_4 Cl (charge = -18) the loading increased roughly 2.5 times when compared to that of unmodified GOx. This increase in biding continued to a net charge of 0 and +35 on the GOx derivatives, with a maximal improvement of 420% when compared to that of GOx, and then the loading began to decrease slightly but measurably to ~320% at maximum charge of +78. PCM, therefore, strongly influenced the binding of modified GOx to GO.

In an independent experiment, we investigated the influence of PCM on the surface potentials of GO/GOx bio-hybrids (**Figure 2.1B**). Consistent with the above binding data, the zeta potential of GO (-40 ± 5 mV) increased to more positive values upon protein binding and the net potential raised to zero for GOx(0) and GOx(35). Neutralization of the negative charge on GO is clearly seen as the net positive charge on the GOx derivative increased steadily. Further increase in charge of GOx increased the surface potentials with an overall charge of +10 for GOx(78). Therefore, successful PCM of GOx leads to roughly 4-times greater loading and surface charge reversal at EGI.

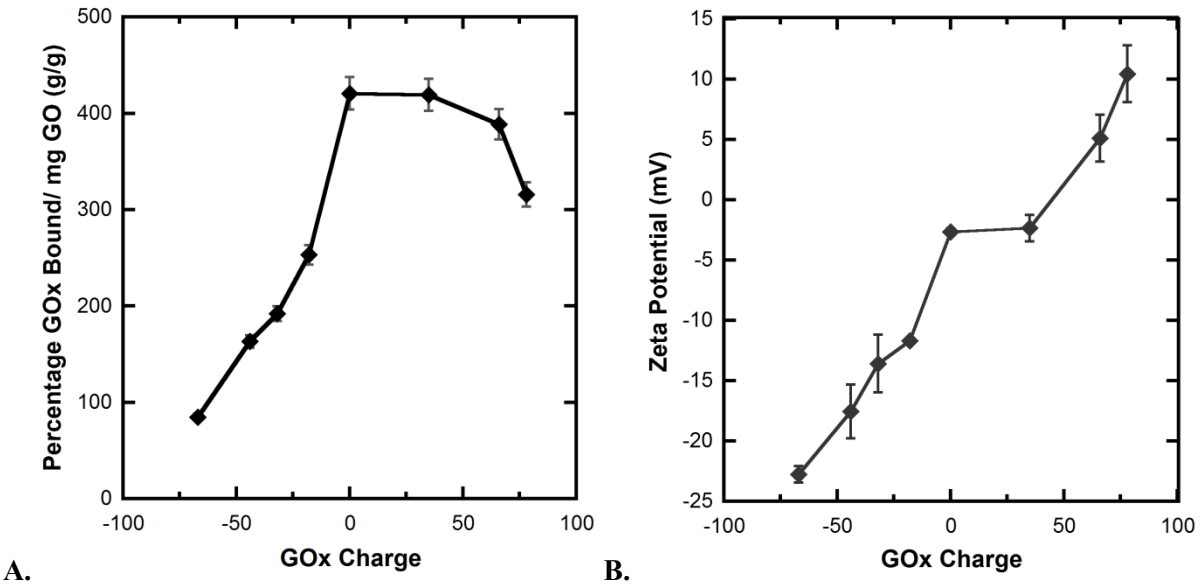

Figure 2.1. Interaction of 4 μM GOx derivatives to 0.15 mg/mL GO in 10 mM sodium phosphate buffer as measured by (A) equilibrium binding studies and (B) changes in the zeta potential upon binding.

2.3.3 Morphology of GO/GOx Bio-hybrids

Based on the amount of protein bound, the total protein footprint on the surface of GO sheets can be calculated. Using the cross-sectional diameter of the GOx dimer, calculated at ~5020 $Å^2$, the amount of coverage by adsorbed protein to the GO surface was determined. Under the assumption that the chemical modification does not contribute significantly to an increase in size of the protein, at the optimum charge range where 99.9% of protein is bound, there is roughly 100% GO surface area coverage by the modified enzyme at charges 0 and 35 (**Table 2.2**).

The maximum amount of unmodified GOx bound showed that it is only capable of utilizing 22% of available surface area of GO in solution whereas highly charged derivatives showed almost 95%. Conveniently, the thin GO nanosheets can be viewed by transmission electron microscopy to evaluate the morphology of GO/GOx samples. GOx (0) was chosen to be loaded onto GO and be analyzed due to the high surface area coverage that was just expressed. The GO nanosheets (**Figure 2.2A**) indicated protein binding as dark spots (**Figure 2.2B, 2.2C**). TEM images clearly indicate that there is no particular ordering of GOx (0) on the GO sheets but rather an evenly dispersed protein layer along the surface.

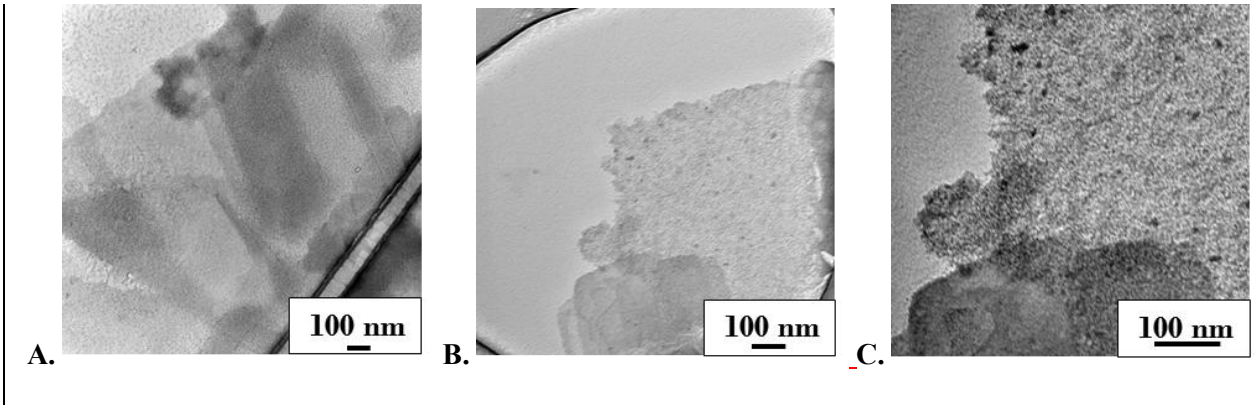

Figure 2.2. Transmission electron microscopy micrographs of 4 μM GOx(0) bound to 0.15 mg/mL GO nano sheets in deionized water. Panel A shows intercalation of dark protein clusters within multiple stacked GO sheets. Panels B & C denote high protein surface coverage of normally smooth, glassy surface of GO to create irregular, gritty surface of GO/GOx conjugates.

Table 2.3. Calculations of GO surface area coverage by GOx derivatives and estimated number of layers formed on GO as deduced from the loading, the known size of GOx, and surface area of GO.

GOx Charge	Maximum Percent Bound	Percent GO Coverage	Number of Layers
-67	84.8	21	0.2
-44	163.1	42	0.4
-32	192.1	49	0.5
-18	253	64	0.6
0	420.6	107	1.0
35	419.13	107	1.0
66	388.55	99	1.0
78	315.56	80	.8

2.3.4 Analysis of Enzyme Secondary Structure Retention of GO/GOx Bio-hybrids

Adsorption of enzymes and proteins on solid surfaces often results in considerable loss in their native-like structures due to strong unfavorable interactions with the solid surface.[49,73]Therefore, we investigated the influence of PCM in controlling these interactions with the GO surface by CD spectroscopy. Protein secondary structure and changes in the structure can be readily detected by CD spectroscopy.[49] The CD spectra of GO/GOx bio-hybrids made from 4 μM of the GOx charge ladder interacting with 0.15 mg/mL GO in phosphate buffer are shown in Figure 4A. The data show extensive retention of structure for the bound enzymes for GOx(-44), GOx(-32), GOx(-18) while that of GOx(0) was less while the derivatives with charges 35, 66 and 78 showed considerable loss on binding to GO.

The intensities of the peak minimum at 222 nm were used to estimate the extents of structure retention for these samples with respect to that of pristine GOx as 100% (**Figure 2.3**). Structure retention is most comparable to that of the unmodified GOx in charges that range from -44 to -18 where there was no significant loss in the signals that are characteristic of the α-helix. GOx(0)/GO retained 95% of its structure, but further increase in protein charge led to a significant loss to ~60%. Overall, PCM influenced the bound protein structure where charges greater than zero appear to have a strong negative influence.

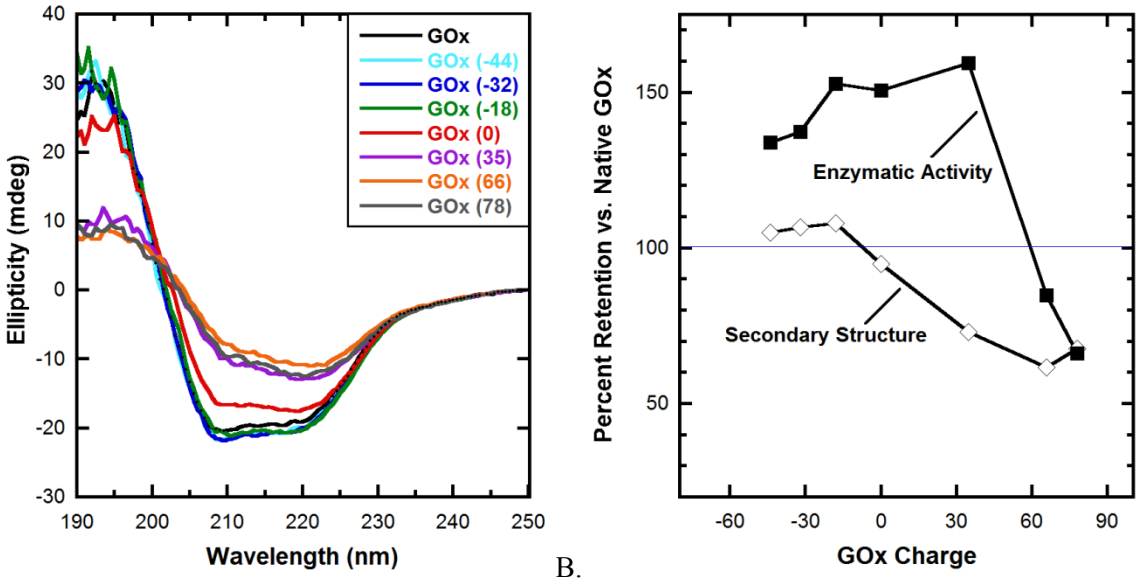

Figure 2.3. Retention of (A) the protein secondary structure, and (B) correlation of the retention of enzymatic activities (squares) with the retention of the secondary structure (diamonds) of modified GOx/GO (4 μM protein, 0.15 mg/mL GO) as a function of charge on the GOx derivative. Solid blue line denotes structure and activity measurements of unmodified GOx under same conditions of pH and iconic strength.

2.3.5 Enzymatic Activities of GO/GOx Bio-hybrids

Enzyme activities are often sensitive to structural loss or changes and binding of the enzymes on the nano sheets could potentially impede their ability to function.[71,73] We addressed these concerns directly in activity studies and evaluated the influence of PCM on the activities of the bio-hybrids. Note that PCM had no significant adverse effect on the activities of unbound GOx derivatives or their structures but this could change once the enzyme is bound to the solid surface. The oxidase activities of 1 μM of these samples after binding to GO were monitored by using methods developed in our laboratory.[49] Specific activities of the samples are presented in **Figure 2.4A**. To our surprise, the specific activities of the bio-hybrids increased when compared to that of the pristine GOx, and these remained high for GO/GOx(-44), GO/GOx(-18), GO/GOx(0), and GO/GOx(30) but samples with charges 66 and 78 indicated a substantial loss. The highly charged derivatives showed some loss in structure and hence, we compared if there is any correlation between the structure retention and activity retention for the bio-hybrids.

The activities and structure retentions of the bio-hybrids relative to native, unmodified GOx are compared directly in **Figure 2.4B**, and they show that activities are maximized at an enzyme charge of +35 while the structure is maximized at an enzyme charge of -18. Thus, the trends are roughly the same, some correlation is seen, but there are significant deviations in the most favorable charge for structure *vs* activities. Thus, PCM turned out to be a powerful tool to not only control biding to GO but also to enhance the enzymatic activities of the bio-hybrids beyond what the natural enzyme is capable of.

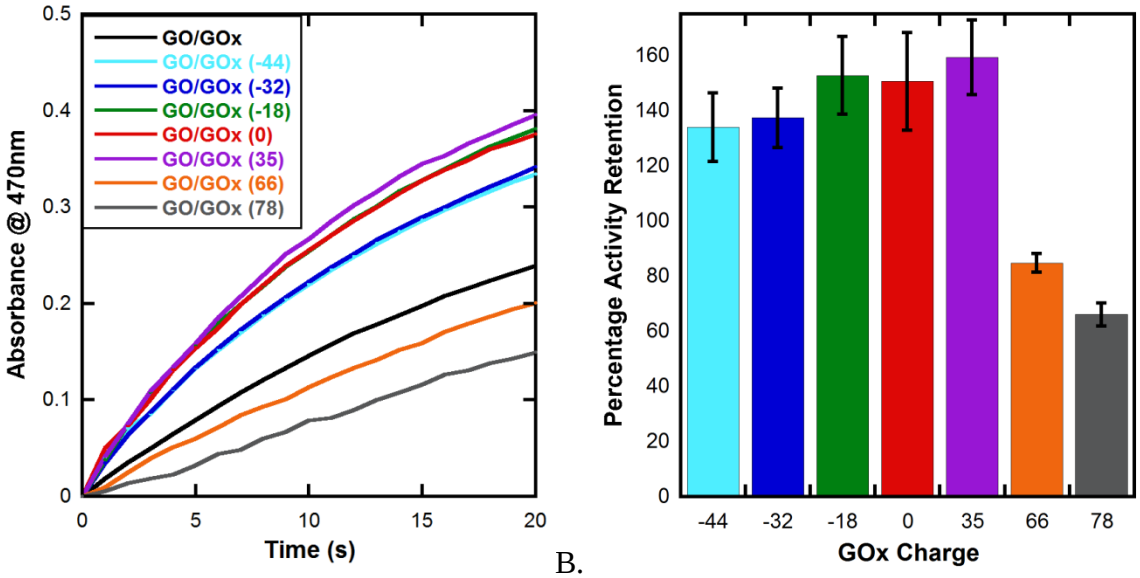

Figure 2.4. (A) Comparison of activities of 1 μM GOx (black line) and GO/GOx samples. (B) Percentage activity retention of GO/GOx derivatives based on charge relative to native GOx. All activities were taken at room temperature in 10 mM phosphate buffer pH 7.0. Color scheme of samples matches that described in **Figure 2.3**.

2.3.6 Influence of PCM on the Thermal Stabilities of GO/GOx

Previous reports from our laboratory suggested that enzyme stability can be improved by intercalation in layered materials but the influence of surface functions of the enzyme on the stability is yet to be evaluated. As temperature is increased, the enzyme structure may unravel and result in loss of activity. Therefore, we examined the catalytic activities of the bio-hybrids (GOx, GOx (0), GO/GOx and GO/GOx (0)) as a function of temperature, from 25-75 °C (**Figure 2.5)**. It was shown in **Figure 1.8** that GOx remained catalytically active at temperatures below 60 °C and that GOx(0) displayed enhanced resistance to thermal deactivation with activity at temperatures less than 70 °C. By binding GOx to the flexible GO nanosheets, the unmodified GOx sample displayed a slight increase in thermal stability, increasing its activity by 5 °C to 65°C. PCM combined with the binding to GO enhanced the thermal stability of GOx(66), which is the positively charged derivative closest in charge to that of the native, negatively charged GOx from 65 to 70°C, but did not result in higher thermal stability in GOx(0), which remained at 70°C as an inactivation temperature. By comparing all samples to those of **Figure 1.8**, a noticible curve shift to a higher temperature can be observed in the case of GOx and GOx(66), but the thermal degradation curve of GOx(0) is roughly the same with the slopes of the lines at 50% activity retention within 0.02 units of each other. This shows that although there is binding of GOx to the GO surface, the nominal thermal insulation properties of GO cannot be transferred to the enzyme at temperatures exceeding the theoretical denaturation barrier.

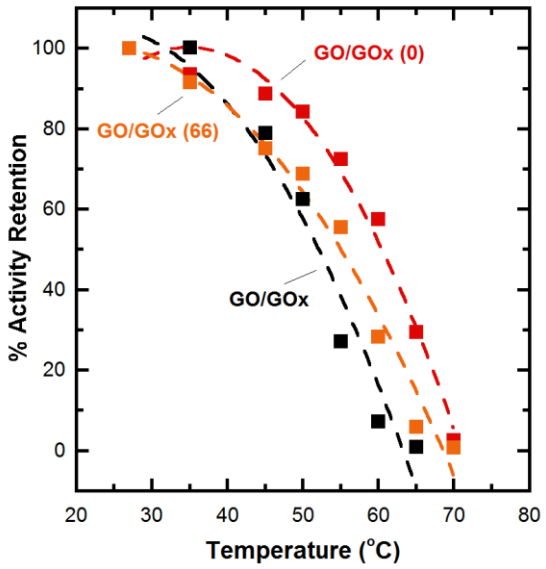

Figure 2.5: Thermal stability studies of 4 μM GOx derivatives (A) and 4μM GOx derivatives bound to 0.15 mg/mL GO (B) in 10 mM phosphate buffer, pH 7.0. Activity retention based on initial rate after 15 minute incubation time at denoted temperature is recorded. All samples were immediately cooled to an internal temperature of 4 °C then re-equilibrated to room temperature to perform all activity studies under same overall temperature after heating.

2.3.7 Kinetic Stability of GO/GOx Bio-hybrids at Biologically and Mechanistically-relevant Temperatures

For practical applications of the bio-hybrids it is crucial that they be stable at or above room temperature for extended periods of time. Therefore, we examined the influence of PCM on the half-lives of the GO/GOx samples at 40 ˚C, tropical room temperature. The higher than normal storage temperature of ~ 4˚C also allows for accelerated aging of the samples, so that the experiments could be completed in reasonable lengths of time. The half-life of GOx, that is the time required for the sample to lose its activity by half, at 40 ˚C is reported to be 30 minutes[64] and we used this as a benchmark to compare the chemically modified GOx samples and their corresponding bio-hybrids at 40 ˚C.

Enzymatic activities of the samples were assayed as before, except that the samples were maintained at 40 ˚C and aliquots of samples withdrawn periodically for testing their activities. Specific activities of the GO/GOx bio-hybrids are plotted as a function of time of incubation at 40 ˚C (**Figure 2.6**), and the time required to reduce the initial activity by half (half-life) has been estimated directly from these plots, in a model independent manner (**Table 2.3**).

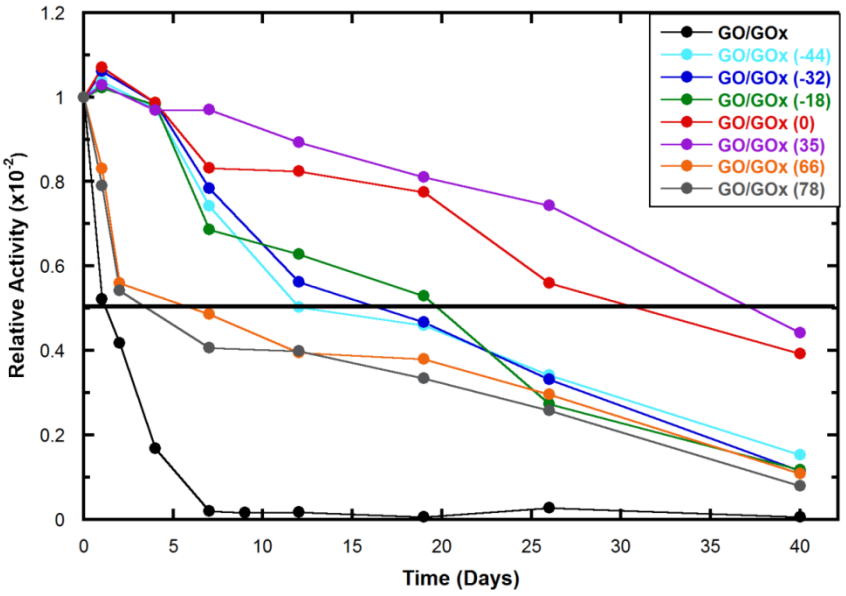

Figure 2.6. Plots of specific activities of GOx charge derivatives bound to GO relative to initial activity of GO/GOx derivative as a function of storage time in days. 4 μM PCM GOx in 10 mM phosphate buffer at pH 7.0 were stored in absence of substrate with and without 0.15 mg/mL GO at 40 °C. Aliquots were taken periodically, equilibrated to room temperature, and activity was measured in triplicate. Initial rates for each derivative were averaged and relative activity to the initial measurement before incubation was compared.

Table 2.4. Calculated half-lives of 4 μM PCM GOx derivatives and PCM GOx derivatives bound to 0.15 mg/mL GO in 10 mM sodium phosphate buffer, pH 7.0. Time at which half of enzymatic activity was retained was estimated from displayed first order decay of enzyme activity over time at 40 °C.

GOx Charge	GOx Half-Life (Days)	GOx + GO Half-life (Days)
-65	0.26	1.55
-44	3.51	18.3
-32	3.79	20.1
-18	4.02	20.3
0	5.63	32.6
35	5.46	38.7
66	4.04	3.35
78	3.67	2.21

Surprisingly GO/GOx conjugates showed remarkable increase in the half-life over several weeks (**Figure 2.7**), and GO/GOx had six-times the half-life of unmodified, unbound GOx. Both GO/GOx(0) and GO/GOx(35) indicated greater than 21-times higher longevity when compared to that of GO/GOx and over 125-times greater than that of GOx at 40°C, holding their activities above 50% of their initial activities for greater than 760 hours. These results are extremely encouraging, and the half-life of GO/GOx(66) and GO/GOx(78) showed a decrease in half-lives from that of highest values noted above but still longer than that of unmodified, unbound GOx. Thus, PCM had a strong influence in increasing the half-lives of these bio-hybrids and resulted in highest known values.

A trend was noted that as sample charge approached zero, the stability was enhanced greatest. As charge deviated from neutral, either in the positive or negative direction, solution stability appeared to likewise decrease. While native GOx, which at pH 7.0 has a net charge of -67 units lived only 0.26 days (6.25 hours), the next shortest lived samples were GOx (78) and GOx (66) whose half-lives were 3.67 and 4.04 hours, respectively. As previously noted, the net neutral GOx (0) derivative was the longest lived at 40°C with a half-life of 5.63 days. The samples with the next highest longevity were GOx (35) (5.46 days) and GOx (-18) (4.00 days), which also were the closest samples to GOx (0) by comparison of charge. In short, GOx with very high number of charges and very low charges have shown shorter half-life when compared to that of GOx with nearly neutral charge before and after binding to GO.

Previously, we observed similar 'optimum charge-maximum output' phenomena as it pertains to binding, structure retention and activity retention studies. These observations drove us to investigate stability of proteins and protein/GO conjugates under other unfavorable conditions such as increasing concentration of chemical denaturants.

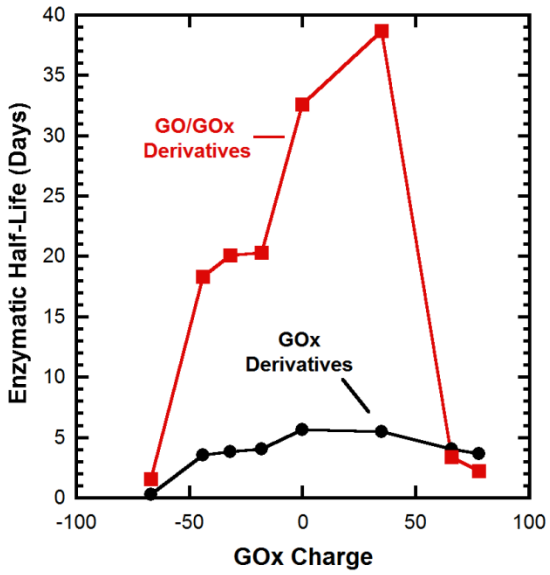

Figure 2.7. Half-life versus charge of PCM GOx derivatives (4 µM protein, black line) and GO/GOx derivatives (4 µM protein, 0.15 mg/ml GO, red line). GO/GOx(35) displayed >150 times increase in half-life at 40 °C when compared to that of unmodified, unbound GOx maintained under identical conditions.

2.3.8 Calculation of inactivation energy of GO/GOx Bio-hybrids

The inactivation kinetics of GOx and GO/GOx derivatives were studied in accordance with the absolute reaction rate theory to dictate inactivation barrier (E_a) and the free energy of intermediate state.[65] The first order decay of enzymatic activity of GOx at 40°C was used to estimate half-lives ($t_{1/2}$) of the enzyme conjugates, thereby the free energy of activation (ΔG^*_{inact}) and the energy of activation (E_a) can be calculated using Equation 1 and Equation 2, respectively.[66] The half-life of GOx (6.25 hours) was found to increase when bound to GO (37.2 hours) and a correlation with net charge of the protein was noted. Similarly ΔG^*_{inact} of unmodified GOx (24.8 kcal mol^{-1})[66] showed an increase of 1.8 kcal mol^{-1} after modification and further increased significantly in case of charge optimized GO/GOx(35) conjugate (27.9 kcal mol^{-1}, **Table 2**). The energy (E_a) of inactivation barrier for GOx (58.7 kcal mol^{-1}) has showed an increase after PCM and was further elevated by GO binding as consistent with trends in both ΔG^*_{inact} and half-life.

Table 2.5. Summary of kinetic and thermodynamic parameters from investigation of GO/GOx binding and activity.

Sample	Half-Life	Inactivation Rate Constant	ΔG^*	Activation Energy (E_a)
	(Hours)	$k_r \times 10^{-6}\ s^{-1}$	$kcal \bullet mol^{-1}$	$kcal \bullet mol^{-1}$
Glucose Oxidase	6.25	0.301	24.8	58.7
GO/GOx	37.2	5.18	25.9	104.8
GO/GOx (-44)	439	43.8	27.5	249.7
GO/GOx (-32)	482	40.0	27.5	255.2
GO/GOx (-18)	488	39.7	27.5	255.7
GO/GOx (0)	782	24.6	27.8	283.6
GO/GOx (35)	929	20.7	27.9	293.6
GO/GOx (66)	80.4	24.0	26.4	150.0
GO/GOx (78)	53.0	36.3	26.2	125.6

2.3.9 Effect of PCM on the Intrinsic Stabilities of Bio-hybrids

While the enhanced thermal stabilities and increased half-lives are excellent for these samples, we also wanted to learn about the intrinsic stabilities of these bio-hybrids. The denaturation free energies of proteins can be determined by examining the UV CD signals of the sample as a function of increasing concentrations of a chemical denaturant such as guanidinium chloride (GdnCl)[67]. For these studies, we chose the most stable bio-hybrid and compared its stability with that of unmodified, unbound GOx, under the same conditions. The far UV CD spectra were recorded with increasing concentrations of GdnCl (0-6 M) (**Figure 2.8**). The equilibrium analysis of the data using the standard methods of analysis indicated the ΔG for the denaturation of GOx, GOx-TETA (0), GO/GOx and GO/ GOx-TETA (0) were found to be very similar regardless of chemical modification or subsequent binding to GO sheets. Therefore, GO sheets did not provide adequate protection from chemical denaturant molecules or enhance the overall protein chemical stability.

Here, binding and characterization data are shown to clearly relate PCM with various physical and chemical attributes of the enzyme, GOx and its interactions with GO. This strategy led to creation of bio-hybrids that far exceeded both the activities and stabilities of the unmodified, unbound GOx as well as providing unprecedented control over enzyme properties.

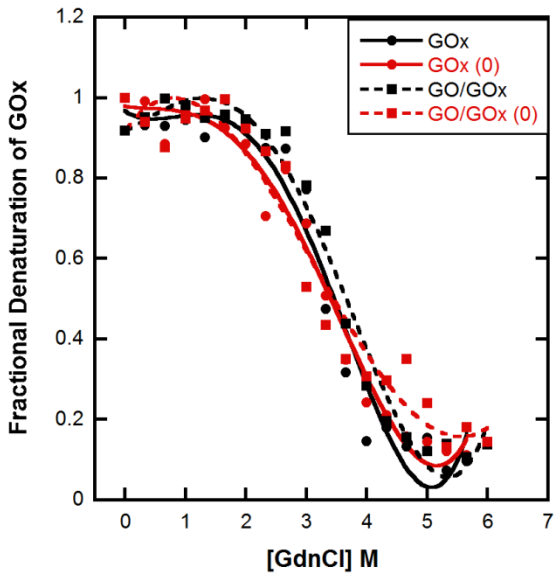

Figure 2.8. Chemical stability of 4 μM GOx (black) and chemically modified GOx derivatives (red), (solid lines) compared with equal concentration of enzymes reacted with 0.15 mg/mL GO (dashed lines) at pH 7 under increasing molar concentration of guanidine hydrochloride. Increased favorability in electrostatic binding to GO surface did not enhance stability under denaturing conditions to a significant extent.

2.4 Discussion

A unique GO/protein biohybrid with unprecedented kinetic stability is presented here. Protein interaction at BGI was controlled by chemical modification of GOx, without altering its structure or activity. At optimum charge conditions binding of modified GOx to GO have shown high affinity in order to produce enzyme rich bionanomaterials with tunable shelf lives of up to several weeks.

Covalent and non-covalent surface modification of GO ranging from small molecules to proteins were employed to modulate its mechanical and electronic properties. [68, 69] Structural deformation of biomolecules on GO surface resulted in poor performance of biological systems indeed overcame by various functionalization approaches.[70] A reverse approach of modifying protein surface instead of GO surface was not established well. We have reported that binding of bovine serum albumin (BSA) to GO could be marginally enhanced by chemical modification with tetraethelenepentamine (TEPA), but binding of biomolecules to the modified GO had an adverse effect on the binding affinity of system .[49] To expand on that work, we studied the effect of number of different amines as the modifier and how the extent of modification effects the affinity of GOx to GO surface. As expected when the number of protonatable amines increased in the modified enzyme, loading was also increased correlating to the overall net charge on the protein. Moreover, based on the electrostatics, one can envision that a polycation can bind to a polyanionic solid better than single charge units due to entropically controlled proximity effects. Since the functional groups on GO are unevenly distributed, the increased flexibility of the modifier also should contribute to the higher binding affinity of the protein.

A large deviation from the aforementioned possible molecular explanation of modified protein binding to GO was noticed when net charge of the protein taken into account. GOx (0) showed an unprecedented increase of 5.3 times the maximum loading of native GOx, the decline in the trend was unexpected and contrary to the electrostatic nature of the BGI. Contrary to the expectations based on classical electrostatic theory, highly charged GOx showed decrease in loading compared to nearly neutral charged derivatives. Zeta potential of the conjugates after protein binding seems to be proportional to the increase in net charge on the protein. Equilibrium binding studies showed that maximum binding of GOx to GO occurred when 4 μM protein had a charge range of 0-35 in pH 7.0 10 mM phosphate buffer. Thus increase in charge is probably due to the protein-dense, highly charged regions on the GO surface.

We noticed that as the charge on GOx increases the tendency of aggregation of the conjugates also increased and those suspensions precipitated after 24 hours (**Figure 2.9**). Aggregation of GO layers due to higher affinity from positively charged proteins outside of the optimum range leads to decreased effective adsorption area, resulting in the trend of lower protein adsorption as charge increases from neutral.

An increase of binding capacity on the GO surface in essence would be useless if that binding were to adversely affect the function of the protein that is being adhered.[71] It has been shown before that highly charged BSA derivatives bound to GO will be denatured forming an amorphous layer of polypeptides coating the surface of GO.[49] Strong interaction of protein with GO has the propensity to cause physical strain to the protein, which then increases the amount of exposed hydrophobic protein residues.[72] Thus, control of interactions at BGI is a challenging task with primary importance in preserving the native functioning of proteins. By finding the

optimum charge matching range of the protein to minimize structural deformation and maintain high activity at BGI we are able to establish greater control of such interactions. Strikingly, high

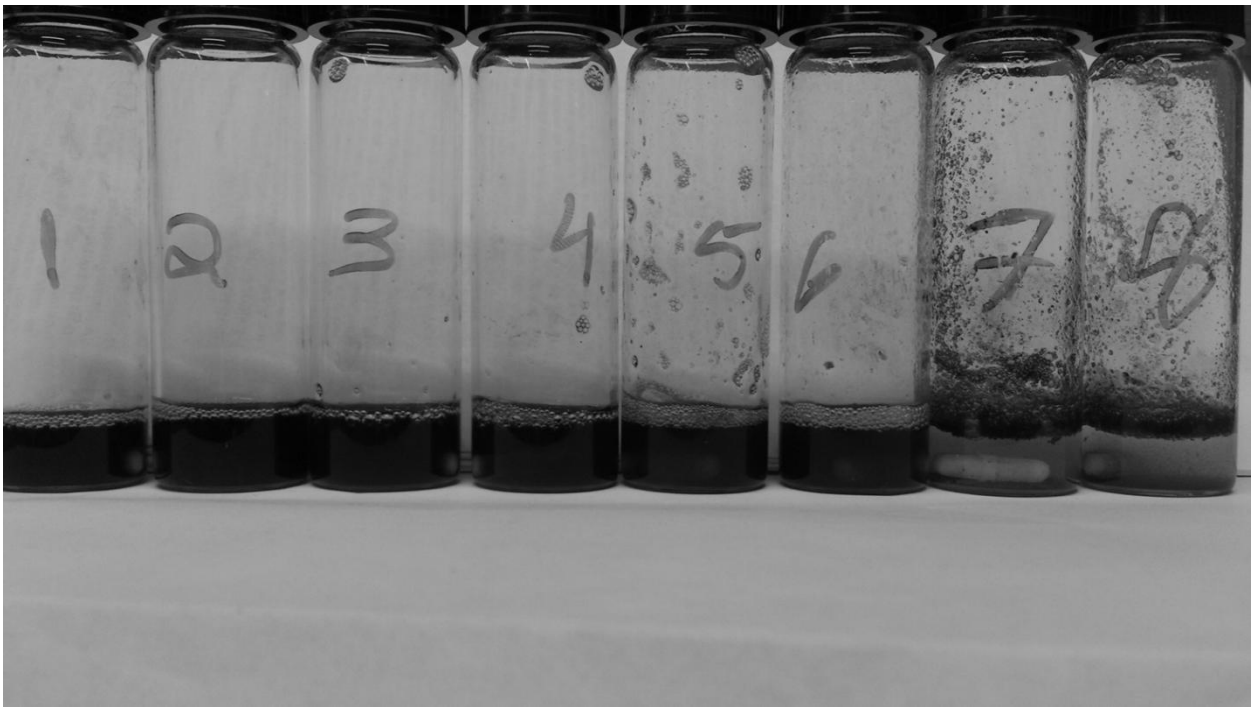

Figure 2.9: GO/GOx conjugates stored for 24 hours at room temperature. Major precipitation was noted for samples 7 (GOx (66)) and 8 (GOx (78)), while all others remained as stable suspensions. Sample numbers correspond to those in **Table 2.1**.

positive charge on proteins had a negative effect on its structure retention and activity prior to the binding. Noticeably, some of our conjugates showed elevated activity compared to that of native free GOx, which is a known phenomenon for other enzymes interacting at BGI.[49,73] As predicted before, this can be seen as a consequence of distortions in the structure of the protein, as shown by CD studies, leading to greater accessibility of substrate to the active site.[74] The possibility of increased electron transfer rate at the redox center, aided by GO, can also account for the increased activity, which is previously observed with various metalloproteins.[75]

The aim of creating GO/GOx hybrids was to combine the mechanically and electronically robust nature of GO with the catalytic functionality of GOx. Testing the conjugates under thermally taxing conditions of increasing temperatures showed that chemical modification of GOx increased its thermal stability after bound to GO by 30% at 65^{o}C, whereas the native free enzyme was inactive. While it can be shown that the native enzyme thermal stability can be increased by the thermal insulation properties of GO, it appears that improved loading onto GO sheets does not further improve the thermal stability of GO/GOx bioconjugates. This increase in activity was not significant compared to an earlier study in regard of trypsin bound to modified GO where the activity was persistent till 80 $^{\circ}$C.55 This observation of low thermodynamic stability was unexpected and brought about thought as to the role of GO sheets in the conjugated system. We chose to test and differentiate between thermal and kinetic stability of the enzyme under the assumption that the 2D sheets may be protecting the protein from thermal inactivation due to constraining the active form of GOx.

At 37 °C, the half-life of GOx has been reported to be around 40 minutes, so we chose 40^{o}C for our studies. The increased temperature led to inactivation of the enzyme in laboratory

timescale. The most significant feature of the GO/GOx conjugates proved to be the substantial improvement in solution storage stability (about 38 days half-life at 40 $^{\circ}$C) which showed a correlation with the surface charge of the protein being in an optimum range. From these half-lives, the energy necessary to deactivate native GOx and GO/GOx derivatives was studied in accordance with the absolute reaction rate theory to determine the free energy of activation.[76]

The propensity of inactivation kinetics has shown a surprising correlation with protein surface charge. A three-fold increase in E_a upon chemical modification of GOx can be seen as a consequence of protein surface charge neutralization leading to relief of columbic strain.[77] Even more astonishing was the magnitude of increase observed in the charge modified GOx samples bound to GO, which displayed E_a greater than 280 kcal mol^{-1} in the cases of GO/GOx (0) and GO/GOx (35). Our thermal stability and chemical stability data shows no significant increase in the thermodynamic state of the proteins. This rules out the probability of increase in stability of the denatured state due to decrease in configurational entropy of the protein upon binding to a 2D sheets. We propose that the native state of the protein has become stabilized by binding to GO sheets, effectively increasing the barrier of inactivation. This is valid based on the assumption that the energy of the intermediate state has been unaffected by binding. As we noticed before, the binding of GOx to GO is driven by the surface charge; the stabilization of the protein native state prior to binding is going hand in hand with electrostatic favorability of binding. Thus PCM appeared to be an underpinning tool to predict and control the kinetics of protein inactivation and no such evaluation has been performed before.

Another pivotal factor leading to the long-lived enzyme conjugates could be the decrease in pre-exponential factor (A) by immobilizing the proteins to 2D sheets. Since the proteins are isolated by the sheets the chances of collision between the molecules are restricted leading to a

decrease in aggregation-induced inactivation of the protein. By adhering the protein to the carbon-based solid, its movement in solution and thereby number of possible collisions in solution is reduced. Therefore, controlled chemical modification of protein along with favorable binding of those modified proteins have the potential to increase their activity and longevity due to reduced number of collisions with other proteins which under normal circumstances promotes aggregation induced deactivation leading to an explanation of the charge dependency on the half-life of protein biohybrids.

The next question to investigate was whether or not the binding of the GOx charge-derivatives to graphene oxide would transfer thermal insulation properties as part of the prolonged longevity of the protein. To determine if there was in fact an induced shielding effect on GOx from thermal inactivation due to its interaction with GO, we verified the structure of the protein using near UV CD studies after 40 days. Strikingly, we found that the structure is roughly 100% correlated to the CD spectra before incubation (**Figure 2.10**). Previously reported increased GOx shelf life was improved on different surfaces and maximum storage life of 180 days at 4^{o}C was reported for GOx covalently attached to gold nanoparticles, although the structure of GOx after binding to gold surface was significantly distorted, and important data as to the storage life was not shown. [78] In our studies we monitored the half-lives at 40^{o}C, which is absolutely necessary for devices or real-life applications where the enzyme would be under such stressed conditions.

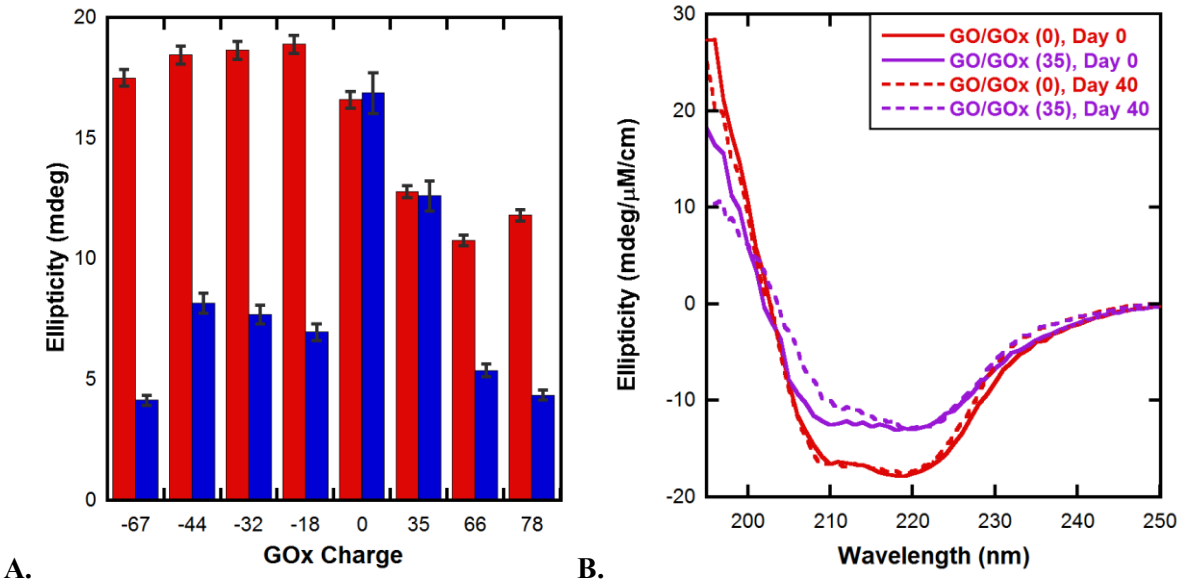

Figure 2.10. (A) Extensive retention of the secondary structure of GO/GOx(0) (4 μM protein,0.15 mg/ml GO) when compared to its initial CD signal. CD intensities of GO/GOx derivatives at 222 nm as a function of enzyme charge after 40 days, maintained at 40˚C (blue) *vs* their corresponding original values before incubation (red). All samples were stored in the absence of substrate in 10 mM phosphate buffer, pH 7.0. (B) Superimposition of the CD of GO/GOx (0) and GO/GOx (35) before (solid lines) and after 33 days at 40 °C of half-life studies (dashed lines)to show comparison of structure retention.

In order to account for the increased rate of inactivation, some key experiments had to be pursued. Stability of proteins under chemically denaturing conditions was performed using GdnCl titration. We observed that increased affinity could not govern any increased chemical stability to the system, which indicates the role of GO as a thermal insulator against thermal inactivation, but not as a protective component to molecules which still have access to proteins on the surfaces of the GO sheets. Another possibility is that GO is acting as a scaffold that accelerates the refolding process of GOx after the heat treatment. Near UV CD data at 40 $^{\circ}$C was analyzed to check the structure of GOx with and without GO proved that even in the presence of GO, structure of the protein had deformed. Thus we conclude that the GO scaffold is not improving the heat resistance of the protein, but rather accelerating the refolding process such that bound protein can return back to native like conformation upon cooling due to the strong electrostatic anchoring effect that proteins at optimum charge experience. In other words, in the absence of GO, the equilibrium state (U) has the potential shift toward both inactive state (D) and native state (N), but confinement of protein structure via GO binding leads to protein stabilized in the N-state upon refolding after subjection to thermal stress. This is in agreement with our thermal and chemical stability data that show GO/GOx composites are not resistant to either heat or denaturants (**Scheme 2.2**)

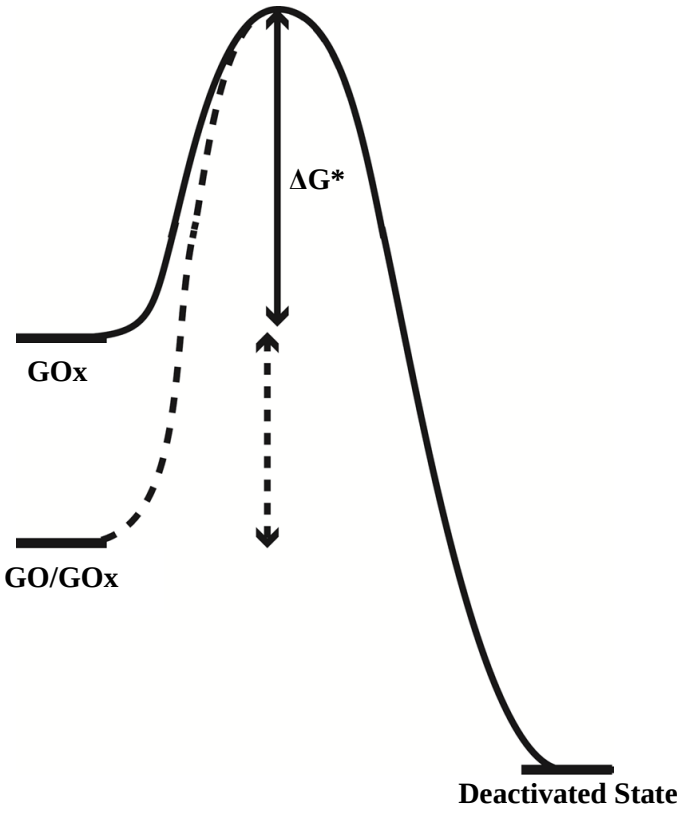

Scheme 2.2. Proposed mechanism of enzyme stability enhancement when bound to surface of graphene oxide. As charge of chemically modified GOx reaches optimum range of binding and interaction with GO, the active state of the enzyme is stabilized, increasing the barrier of energy required for deactivation. Activated complex at peak of barrier is also not deformed due to stabilized state, leading to prolonged activity in enzyme.

The loss of activity despite the conformational retention was puzzling and most likely due to displacement or inactivation of the FAD cofactor that is necessary for the oxidation function of GOx. It is possible that hydrolysis of the phosphodiester group of FAD may have rendered the active site constituent inactive after a certain amount of time or reactions with glucose. Another explanation is that due to thermal annealing of graphene oxide over time in the 40 °C environment, the formation of reduced graphene oxide (rGO) could enhance the hydrophobicity of the surface, which is known to affect the tryptophan reside at the active center of GOx.[72]

2.5 Conclusions

Though chemical modification of the surface of graphene oxide in order to enhance protein or small molecule binding has been practiced, modification of the adsorbate to GO in order to enhance binding is a relatively seldom used approach. A general strategy is described here to systematically control the net charge of GOx by benign alterations to the surface chemistry of the protein without compromising structure or activity of the enzyme, allowing for more favorable binding to highly versatile GO sheets, which is confirmed by equilibrium binding, zeta potential studies and TEM studies.

Modification of GOx with this selective set of ligands show that binding properties to GO are essentially independent of the amine used, but rather depend more driven by surface charge. Surprisingly, an optimum positive charge of the enzymes at physiological pH was required for higher affinity, activity, and structure retention characteristics. GO/GOx conjugates with appropriate charge distribution showed the ability to maintain above 50% activity for more than 30 days. It was also observed that the activation energy barrier and free energy barrier in modified GOx samples bound to GO were enhanced due to restriction of movement and aggregation of the proteins in solution.

Such kinetic stability can prove beneficial to systems such as biofuel cells, whose function depends directly on the chemical reaction that naturally occurring enzymes perform. Super-stable GO/GOx conjugates have the potential to be used for a myriad of applications due to high retention of activity incorporated with unique characteristics of graphene oxide. This facile approach has can be used to successfully control affinity by manipulation of charge of the protein and can be expanded to further applications in bio-nanotechnology.

Chapter 3

Hierarchical Co-Assembly of Chemically Modified Protein/DNA Superstructures

3.1 Introduction

The binding of proteins to DNA has been researched extensively to determine the mechanisms behind gene regulation and expression, replication of DNA chains, and packaging of nucleic acid material within nuclei of cells.[79,80,81,82] There are numerous enzymes that have the ability to recognize specific oligonucleotide sequences and make beneficial repairs to mismatched DNA segments after the replication process.[83] There are also proteins whose interaction is of a more non-specific nature, such as histone complexes used to condense and supercoil long DNA strands.[84] The importance of these protein-DNA interactions have been explained as a combination of the specific and non-specific binding mechanisms, where electrostatic interactions drive binding of proteins to DNA and then allow for sequence-specific recognition to be possible.[85]

Perhaps the most well-known example of protein-DNA interactions is that between histones and double helix DNA to form nucleosomes. The protein core composed of an octomer of histone subunits plays a pivotal role in condensing DNA into the nucleus but also in gene regulation, where select post translational modifications can lead to enhanced or suppressed gene expression.[86] An important characteristic of the histone protein that makes it ideal for DNA wrapping and condensing is that it is highly positively charged with numerous lysine and arginine residues. These residues allow for salt bridges and hydrogen bonds to be formed with the phosphate oxygens on DNA. These electrostatic attractions then allow for strong nonpolar interactions between the histone and the deoxyribose sugars present inside the DNA double helix which stabilize the nucleosome formation.

The interactions between histones and DNA have previously been investigated by optimizing both salt concentrations,[87] as well as mutations to the proteins to maximize the number of surface lysine groups present to interact with the DNA chains.[88] The increased number of lysines will intrinsically increase the positive charge of the histone and thereby enhance the binding potential of the octomer to the DNA. Choosing to mimic this charge-binding theory, we have shown previously that bovine serum albumin (BSA), chemically modified with positively charged triethylenetetramine polyamines, can enhance protein binding to DNA, where the native protein interaction with DNA is very weak.[89] These strong interactions were ideal for creating a light harvesting complex which had the capability of harnessing light energy from 350-670 nm, well above the range of commercial silica based solar cells. The bio-solar cells that our group was working toward would be composed of chemically cationized BSA bound to DNA with fluorescent chromophores bound to hydrophobic patches of BSA as well as intercalated between the nucleic acid bases in DNA. In order to maximize the energy transfer potential of the antenna systems, protein-DNA-dye conjugates were dried in order to increase bulk concentrations within the system and minimize Förster distance between donor-acceptor dye pairs. After the drying process, it was observed that the BSA-DNA mixture had formed organized, crystalline-like structures. Here, we attempt to characterize and investigate the mechanism behind the incredible level of macroscale ordering observed in the interaction of chemically modified BSA with DNA chains.

Living systems consist of functional bio-molecular assemblies in numerous capacities ranging from protein subunits converging on a small scale to perform important tasks such as ATP synthase or ribosomes to larger scale compilations like microtubule chains and virus capsid assemblies.[90] These complicated structures grew to form large structures via spontaneous self-

assembly from smaller molecular components, and have the ability to construct themselves into pre-defined active formations due to strict control of biological cues. While evolution has perfected most of these processes, the natural assembly of large highly ordered biological components still raises many questions to this day especially when it comes to replicating these processes in a laboratory setting.[91] A considerable challenge for researchers attempting to harness the strict control nature has over these processes is that, to date, there is no way to obtain a molecular blueprint for the construction of articificial bio-macromolecule assemblies for light-harvesting.

As a launching point to gain insight into these fundamental issues, we look into what could be the driving force behind the assembly of our observed ordered structures. By utilizing a myriad of imaging techniques such as optical, scanning electron, and atomic force microscopies, we look into how many levels of organization these structures contain. Is it possible that the protein-DNA interactions play a crucial part in the assembly, or is it simple means of surface tension leading to large structural facets? With this preliminary investigation into the mechanism of macroscale assembly formation, we hope to gain unprecedented control over organization of large bio-molecular complexes and use this control to aid in the design of novel biomaterials such as biofuel cells or various biosensors.

3.2 Experimental Procedures:

3.2.1 Chemicals and Materials

Bovine serum albumin was purchased from Equitech-Bio, Inc (Kerrville, TX) and fish sperm DNA was purchased from Amresco (Solon, OH). Glucose Oxidase from *Aspergillus niger*, lysozyme from chicken egg white, and triethylenetetramine were purchased from Sigma-Aldrich Co. (St. Louis, MO). N-(3-dimethlaminopropyl)-N-ethylcarbodiimide (EDC) was purchased from TCI America (Portland, OR).

3.2.2 Chemical Modification of Proteins

Aspartic acid and Glutamic acid residues of Bovine serum albumin (BSA) and glucose oxidase (GOx) were modified using EDC chemistry to activate them with carbodiimide, creating a good leaving group to react favorably with triethylenetetramine (TETA) conjugation to amino acid residue.

BSA modification was carried out by dissolving 1.5 g solid BSA in deionized water and stirred with 0.5M TETA (pH adjusted to 5.2 using concentrated hydrochloric acid) for 30 minutes at room temperature. After initial mixing period, 95.9 mg of EDC was dissolved in 1 mL of DI and added slowly to solution stirring at 600 rpm until final concentration of reaction mixture was 25 μM. The conjugate samples were then stirred at 250 rpm for an additional 4 hours. After synthesis period EDC, TETA, and other byproducts of synthesis were removed by dialysis against deionized water or 10 mM sodium phosphate buffer, depending on experimental

demands. Concentration of dialyzed protein was then analyzed by using molar extinction co-efficient of 43,824 $M^{-1}cm^{-1}$ at 280nm.

GOx modification was carried out by dissolving GOx in deionized water so that the final concentration of the synthesis would be ~6 mg/mL protein. To this, TETA at pH 5.2 was stirred with protein to a final concentration of 25 mM polyamine. After 30 minutes, EDC was added slowly until final concentration equaled 15 mM and stirred for 4 hours according to conditions above. After synthesis and dialysis into DI, GOx sample was concentrated using 50k molecular weight cut-off amicon tubes from Millipore (Billerica, MA). Concentration of concentrated product was then determined by using molar extinction co-efficient of 267,000 $M^{-1}cm^{-1}$ at 280nm or 28,200 $M^{-1}cm^{-1}$ at 450nm (FAD cofactor).

3.2.3 Agarose Gel Electrophoresis

Native agarose gel electrophoresis was performed using horizontal gel electrophoresis apparatus (Gibco model 200, Life Technologies Inc, MD). Molecular biology grade agarose from U.S. Biological (Swampscott, MA) (0.5% w/v), in 40mM Tris-acetate buffer, pH 7.0, was dissolved via heating and then poured into gel apparatus to form casted gel. 8µL of modified GOx samples were combined with 17µL loading buffer (50% v/v glycerol and 0.01% w/w bromophenol blue) and 20µL of samples were loaded into wells at the middle of the gel so that they could migrate toward the negative or positive electrode, depending on the net charge of the enzyme. Running buffer used for all the samples was 40mM Tris-acetate, pH 7. Potential of 100 V was applied for approximately 30 minutes at room temperature. Gels were stained overnight with 10% v/v acetic acid, 0.02% w/w Coomassie blue, and destained in 10% v/v acetic

acid, overnight. Gels were photographed using a BioRad Molecular Imager Gel Doc XRS System.

3.2.4 Zeta Potential Measurements

Protein surface charge was analyzed by using ZetaPlus Zeta Potential Analyzer from Brookhaven Instruments Co. (Holtsville, NY). 300 μM chemically modified BSA suspensions in 10 mM sodium phosphate buffer at pH 7.0 were equilibrated to room temperature and electrophoretic mobility of the samples (1.6 mL) was measure in a polystyrene cuvette (4 mL). Zeta potential values in mV were calculated using Smoluchowski fit provided by the manufacturer.

3.2.5 Optical Microscopy imaging

Samples containing 0.3 mM BSA_{TETA} (+27) and 0.8 mM fish sperm DNA (fsDNA) in total volume of 1 mL were drop casted onto a glass cover slip (Fisher Scientific) and allowed to dry 24 h in standard laboratory fume hood. Samples also contained 75 μM Fluorescein from Sigma (St. Louis, MO), which is known to bind to hydrophobic pockets of BSA[92] in order to enhance light refraction and visualization. Images were then captured using Canon EOS Digital SLR Camera.

3.2.6 Scanning Electron Microscopy (SEM) imaging

0.3 mM BSA_{TETA} (+27) was combined with 0.8 mM fsDNA in 1mL of pH 7.0 Hydro Nanopure distilled water. 500 μL of the suspension was drop-casted onto a Fisherbrand ® 22 mm^2 microscope silica cover slips (Fisher Scientific). Samples were covered and allowed to

dehydrate for 24h at room temperature in the laboratory fume hood. Dried specimens were then gently rinsed with Nanopure distilled water and allowed to further air-dry overnight as above. This was followed by a light coating of the samples, under vacuum, of gold-palladium with Polaron Sputter Coating System. SEMs were performed using JEOL JSM-6335F Field Emission Scanning Electron Microscope and photomicrographs were taken at particular magnifications as denoted

.

3.2.7 Energy Dispersive X-Ray Spectroscopy (EDXS) studies

EDXS was performed on SEM samples using JSM-6335F cold cathode field emission SEM equipped with Thermo Noran System (JEOL USA Inc, Peabody, MA). Accelerating voltage and probe current were set to 10 kV and a dead time of 9 μs, respectively. Using scanning range control, elemental composition was determined by monitoring Oxygen (O) Phosphate (P), Carbon (C), and Nitrogen (N) in the samples within a well-defined area of the viewing micrograph. Averages of 3 trials of scanning over the desired area were recorded.

3.2.8 Powder X-Ray diffraction studies

BSA_{TETA}/fsDNA suspensions (in 10 mM sodium phosphate buffer) were drop-casted on glass slides and air-dried over 2 days. The powder XRD was recorded on Rigaku Altima IV diffractometer (Woodlands, TX) with CuKα radiation (λ = 0.15406 nm) at the beam voltage and the beam current of 40 kV and 44 mA, respectively. Each sample was scanned at a continuous scan rate of 1º /min.

3.2.9 Atomic Force Microscopy (AFM) studies

Atomic Force Microscopy was used to determine the surface morphology of molecular assembly constructs to a very high level of resolution. AFM was performed using Veeco MultiMode SPM on BSA_{TETA}/fsDNA fibrous assemblies. BSA_{TETA}/fsDNA (0.3 mM protein, 0.8 mM DNA) was dropcasted onto glass slide and allowed to dry 24 hours in laboratory fume hood. After drying process, two fibrous strands of dried film were removed carefully and placed on bare mica surface. 2 μL of HPLC grade distilled water was added to mica in order to adhere fibers and ensure they would stay in place as cantilever analyzed surface of sample. After drying of water on surface was completed, samples were carefully placed onto AFM sample deck for analysis.

3.3 Results

3.3.1 Chemical modification of proteins

Bovine serum albumin and glucose oxidase used in this study have isoelectric points of 5.5 and 4.6, respectively, and therefore will be negatively charged at pH 7. At this pH, the negative charge characteristic of both proteins will lead to charge-charge repulsion with the phosphate backbone of DNA. Aspartic acid and glutamic acid residues on BSA and GOx surfaces were conjugated successfully with triethylenetetramine (TETA) using EDC chemistry. Surface charge reversal of BSA was monitored using agarose gel electrophoresis, where the protein is subjected to an external electric field. Distance of migration of the protein samples in the native gel is proportional to the charge of the protein (**Figure 3.1**) and the effect of the change in protein size is minimal. At pH 7, the negative charge of unmodified BSA and GOx leads to the migration of the pristine enzymes toward the positive electrode. After chemical modification with TETA the protein migrated towards the negative electrode, signifying successful charge reversal from negative to positive. Modified samples will be denoted as BSA_{TETA} for convenience.

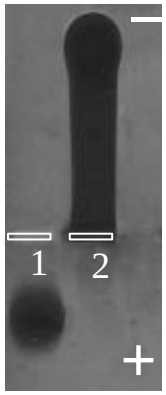

Figure 3.1. 40mM Tris-Acetate agarose gel (pH 7.0) of native BSA (lane 1) and charge modified BSA after EDC chemistry reaction to conjugate reactive amine group to surface carboxyl functional groups (lane 2).

3.3.2 Zeta Potential studies

In order to confirm protein surface charge was being modified, zeta potential measurements were made under conditions of low ionic strength. Upon interaction with the electric field, it was shown that the protein in solution registered zeta potential value of +24.5 mV with a standard deviation of ± 2.85 mV (**Figure 3.2)**. To determine how dispersed charge within the system was, the half-width of the zeta potential peak was analyzed and determined to be 3.94 mV, equating to 16% heterogeneity in the sample. Therefore, 84% of the 0.3 mM BSA_{TETA} sample was determined to be within range of the 24.5 mV charge.

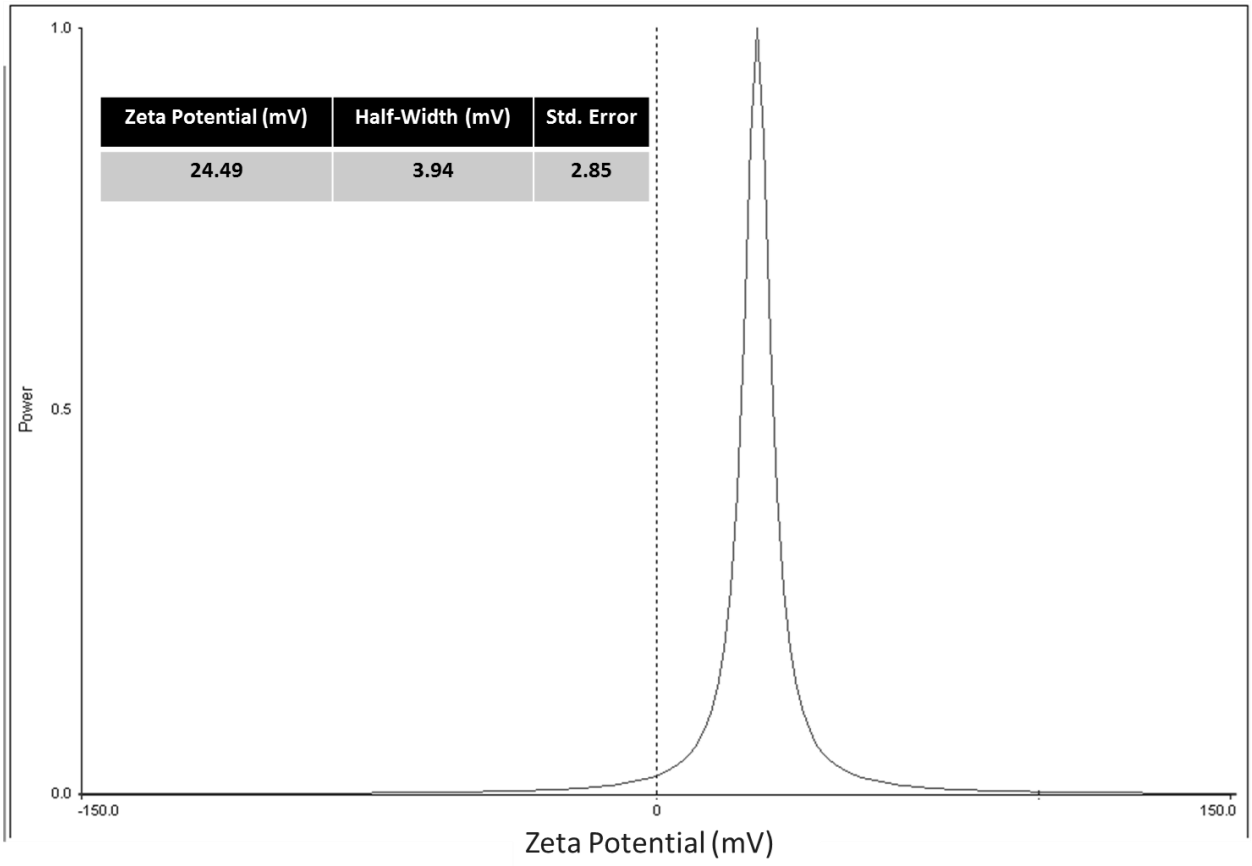

Figure 3.2. Zeta Potential measurement of 300 μM BSA_{TETA} in solution at pH 7.0 in 10 mM Phosphate buffer. Addition of triethylenetetramine functional groups via an amide bond after EDC chemistry reaction change net charge of protein molecules to ~24.5 from a native charge of ~ -30.

3.3.3 Optical Microscopy

Drop casting of BSA_{TETA}/ DNA complexes onto glass slides was performed previously in order to maximize protein, DNA, and dye concentrations of the Artificial Antenna Complex (AAC). When the protein solution was combined with fsDNA stock solution, the addition did not cause any type of precipitation or visible aggregation of the sample. After the drying period, it was noticed that film had formed into long, linear structures which appeared to be incredibly uniform. The glass cover slip that the films had been casted on proved to be ideal for visualization of these linear structures using optical microscopy. To enhance resolution of the images, fluorescein dye was added into the protein solution and equilibrated for 30 minutes before the addition of DNA.

Under the optical microscope the morphology of the BSA_{TETA}/ DNA structures indeed proved to have a high level of organization (**Figure 3.3**). Macrostructures of the protein/ DNA assemblies were on the order of millimeter length scale. Even more surprising than the strand formations was the uniformity of the width between each individual strip. Each "floorboard" like BSA_{TETA}/ DNA complex that formed was spaced 0.005 mm from the other, showing distinct organization characteristics. Optical microscopy images also gave the impression that the samples were forming sharp-edged, crystalline-like structures upon drying.

A. 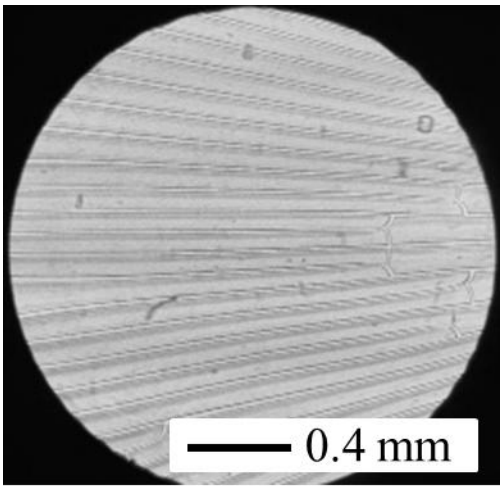

B. 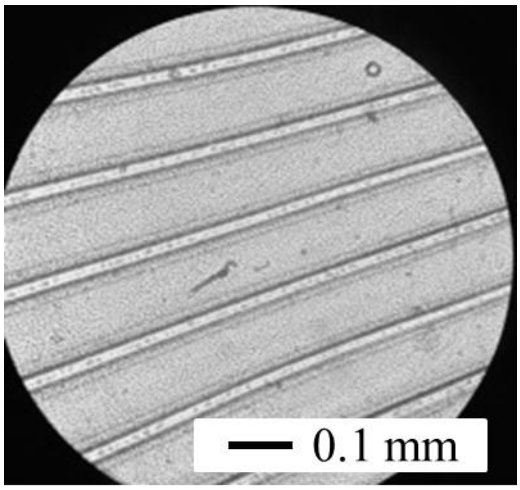

Figure 3.3. Optical microscopy of supramolecular assemblies made from 300 μM BSA_{TETA}/ 800 μM fsDNA dissolved in HPLC grade deionized H_2O casted onto glass cover slip and dried over-night at room temperature. Highly organized structures can be observed on mm length scale with exceptional uniformity from both 100x (**A**) and 400x (**B**) magnification.

3.3.4 Scanning Electron Microscopy

The high organization that was confirmed using optical microscopy led to the attempt to further view the structures at higher magnification than the optical microscope would allow. TO achieve this, we chose to use scanning electron microscopy (SEM) to view our samples. SEM has the potential to resolve samples to better than 200 nanometers, which could help us understand better the composition of the macrostructures we were viewing.

One drawback of SEM technique, however, is that these samples are carbon-based biological samples. The main elements of the BSA_{TETA}/ DNA structures (carbon, oxygen, nitrogen, phosphate) would not give a quality signal to achieve resolution higher than that of the optical microscope. To combat this issue, the protein/ DNA films were lightly coated with gold-palladium particles in order to increase conductivity of the sample. This would allow for the focused beam of electrons from the SEM to have a stronger interaction with the biological samples we wished to characterize.

By inducing a slight tilt to the samples, the secondary electrons of the coated BSA_{TETA}/ DNA samples once again showed highly organized structures (**Figure 3.4**) as seen under optical microscopy. Under low magnification it is clear that there are hundreds of large aggregates present on the order of hundreds of microns long with a very high order on these length scales (**Figure 3.4A**). These long, highly organized structures again displayed unique uniform spacing characteristics ranging from 5-8 μm in length between each 'floorboard' of protein/ DNA

complex (**Figure 3.4B**). The enhanced resolution that we hoped to gain from using the SEM proved beneficial, leading to the first views of highly resolved surface morphology of the BSA_{TETA}/ DNA structures. Whereas lower magnification in both optical and scanning electron microscopies gives the visualization that the structures we are viewing are smooth surfaces,

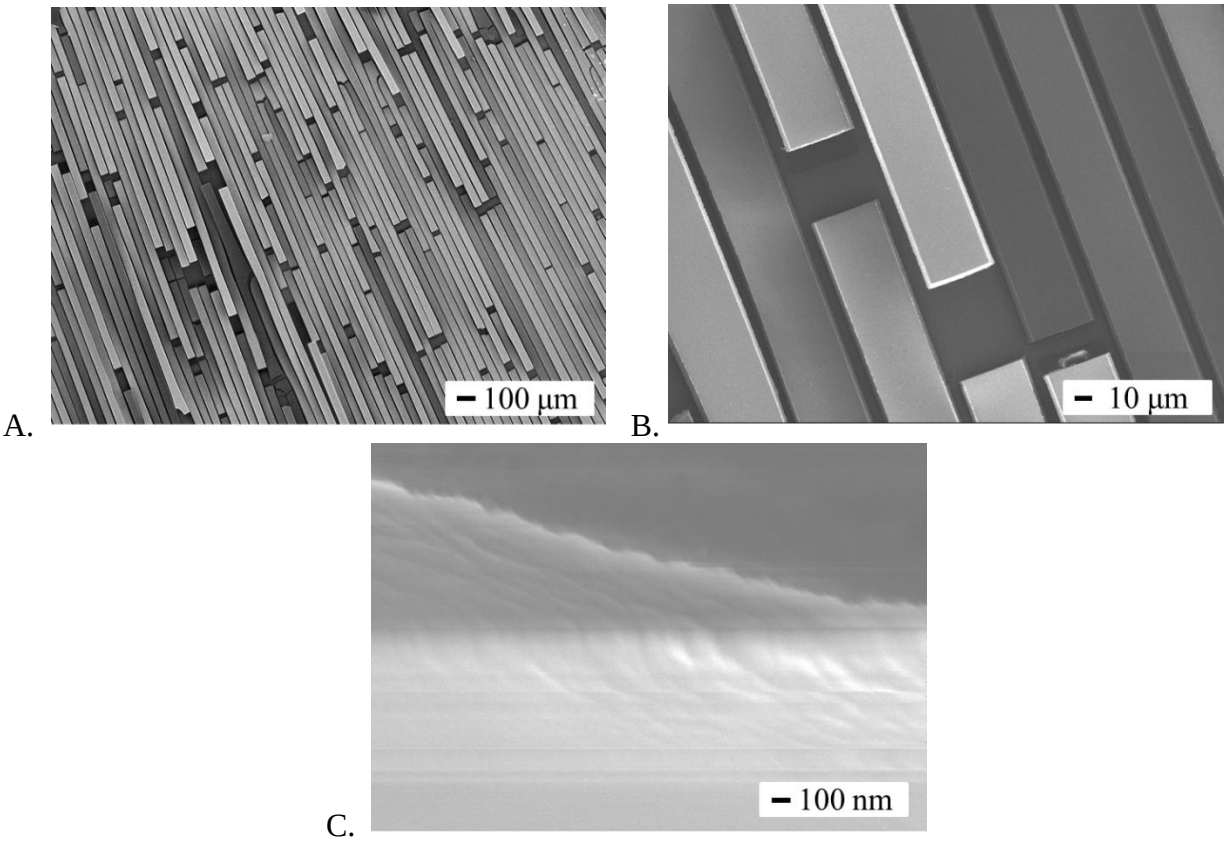

Figure 3.4. Scanning electron microscopy (SEM) micrographs of 300 μM BSA_{TETA}/ 800 μM fsDNA dissolved in HPLC grade dH_2O, drop-casted onto glass cover slip and dried at room temperature overnight. High degree of organization and uniformity that was observed in optical microscopy also apparent on scale of hundreds (**A**) and tens of microns (**B**). Surface morphology (**C**) also appears to demonstrate multitude of molecular structures organized in single linear fashion.

magnification of 30,000X shows that the physical make-up of these samples is rather rough and disorganized (**Figure 3.4C**).

To determine whether or not this phenomenon was dependant on the protein or DNA for the highly organized structures, SEM was also performed on each of the individual components for analysis. BSA_{TETA} was concentrated and washed with 6 rounds of HPLC grade water via centrifugation and 25K MWCO Amicon tubes from Millipore. After the concentrating and washing process, the protein sample was resuspended in DI to a concentration of ~2 mM. 0.5 mL of 300 μM BSA_{TETA} was dropcasted onto the glass coverslip and allowed to dry overnight according to conditions outlined previously. Samples were coated with AuPd and analyzed in the SEM using an accelerating voltage of 5.0 kV. Samples of only BSA_{TETA} showed similar charachteristics when as it pertains to sharp crystalline-like structures, however were noticibly shorter in length than the BSA_{TETA}-DNA assemblies (**Figure 3.5A**). While the majority of the structures containing the modified protein and DNA together had length on the scale of millimeters, only BSA_{TETA} had an averae length of 0.1 mm.

800 μM fsDNA was also measured under SEM after coating with AuPd. Without the presence of protein the DNA displayed feather-like structures devoid of the long scale organization present in the bioconjugates (F**igure 3.5B**). While BSA_{TETA} maintained what appears to be the majority of the structure except for the length, DNA alone does not display characteristics of organized block formations. One result that should be noted though is the

length scale of the DNA samples is more than ten-fold that of the protein by itself, on the range of tens of millimeters.

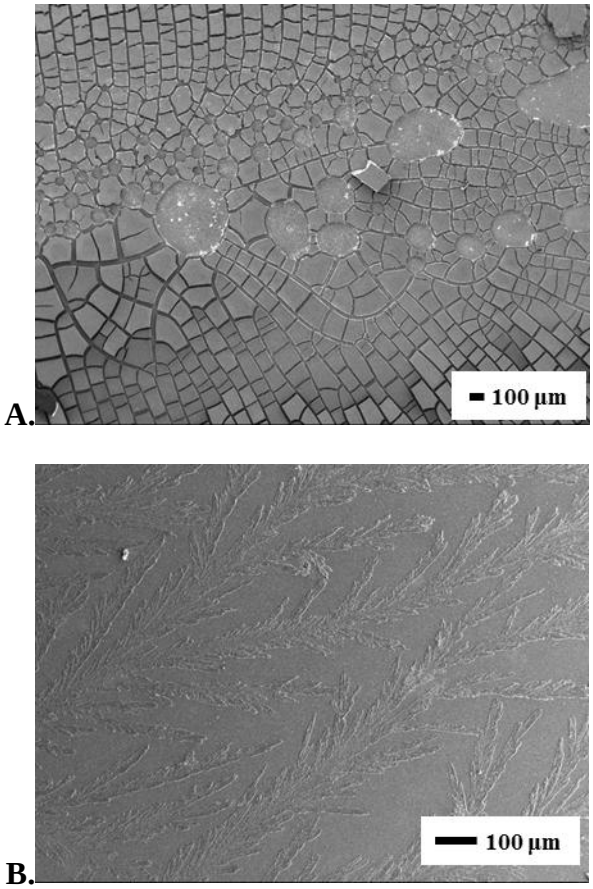

Figure 3.5. SEM micrographs of 300 µM BSA_{TETA} (A) and 800 µM fsDNA (B) dissolved in HPLC grade DI and drop casted onto glass cover slip. Samples were air dried overnight in laboratory fume hood at room temperature before coating with gold-palladium for analysis.

3.3.5 Elemental Analysis of BSA_{TETA}/ DNA films

The composition of the macromolecule constructs that resulted from the interaction of chemically modified BSA and DNA were examined by EDX, to gain insight into the organization of these large scale molecular constructs. SEM micrographs of BSA_{TETA}/ DNA at 2,300X magnification (**Figure 3.5B**) show rough constructs of the superstructures as being proliferous. Elemental analysis of an individual sample area of the molecular super structures showed that it had highest elemental composition of Carbon, Oxygen, Nitrogen, and Phosphate (**Figure 3.5C-F**, respectively) which are also the major components of both the protein and DNA used as the precursors to the film formation. The EDX studies were performed in the absence of any buffer to rule out contribution from any other salts or ions that may contribute to the formation of the structure.

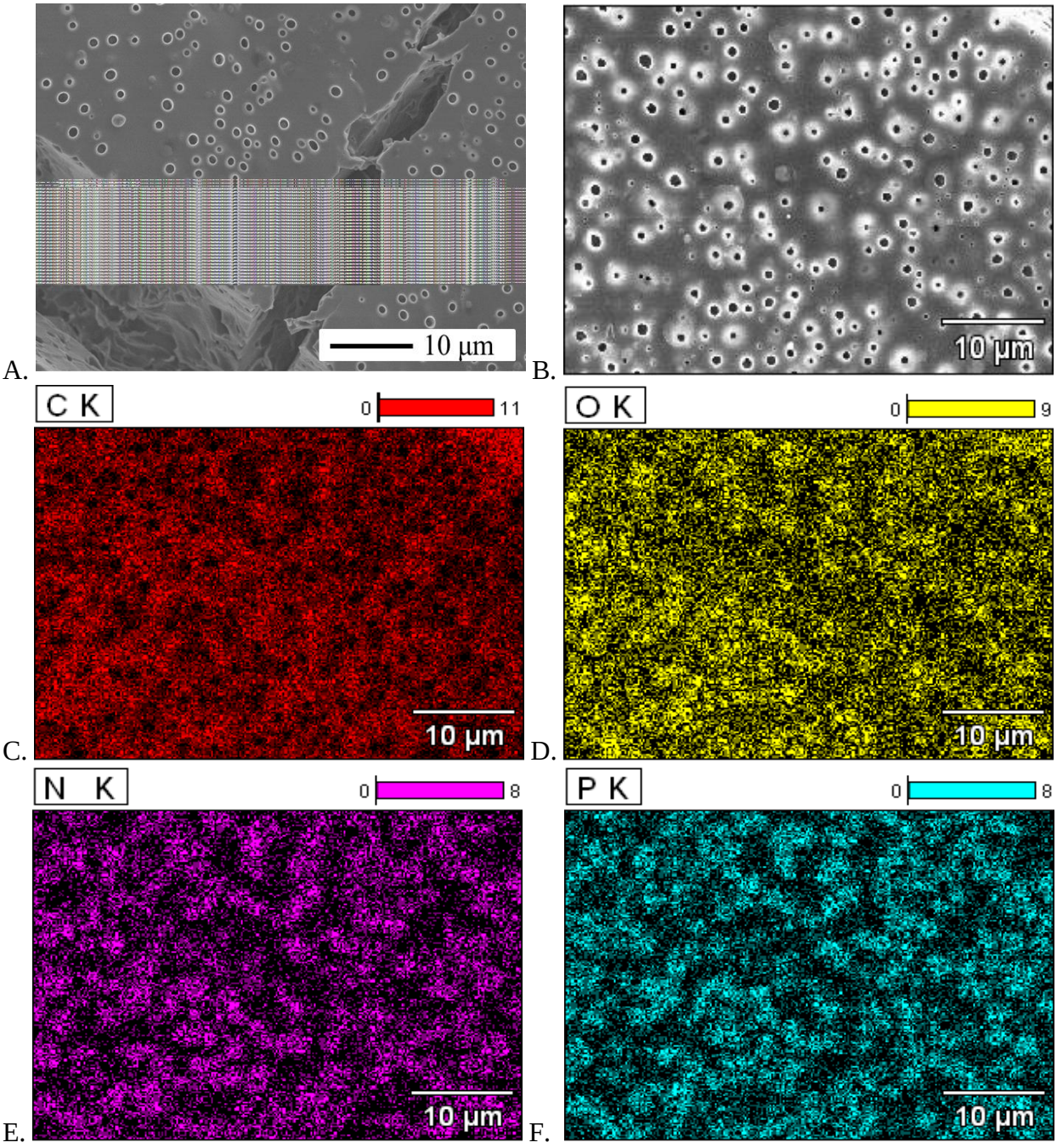

Figure 3.6. Elemental analysis of 300 µM combined with 800 µM fsDNA in HPLC grade dH_2O (**A**, **B**) displaying composition of molecular assemblies is in fact combination of biological polymer components carbon (**C**), oxygen (**D**), nitrogen (**E**), and phosphorous (**F**). No discernable order of elements is visible at the high magnification, leading to belief that protein-DNA binding is random at molecular level.

3.3.6 Atomic Force Microscopy

The notably rough surface texture seen in scanning electron microscopy was extremely interesting, leading us to pursue atomic force microscopy (AFM) to determine the true surface morphology of these macroscale biological assemblies. By carefully removing two linear structures from distinct locations of the dried BSA_{TETA}/ DNA film with transmission electron microscopy tweezers, the cantilever of the AFM was able to scan the surface of these two large scale structures.

The AFM showed that these two structures were in fact not flat, two-dimensional structures, but in fact 3-D assemblies with a height (z-axis) of roughly 200nm (Figure 3.5). Upon further analysis, it was shown that the surface of the individual superstrucrues was composed of what appeared to be numerous fibers running lengthwise along the linear formation (Figure 3.6). These newly discovered fibers were analyzed using both 2D and 3D angles of the structure and were found to have dozens of smaller linear striations running parallel to the larger structure, which was visible to the naked eye.

Using the high-resolution capabilities of the AFM, it was determined that the smaller linear striations composing the superstructure were on a scale of tens of micrometers in length, while only being ~2 μm in width (**Figure 3.7**). Each of these microfibers was then analyzed to determine their individual height, which was determined to be between 5-10 μm. As previously shown in **Figure 3.4B**, the total width of the BSA_{TETA}/ DNA superstructures was ~30 μm. We believe that this meant that we were viewing smaller fibrous subunits of the overall superstructure.

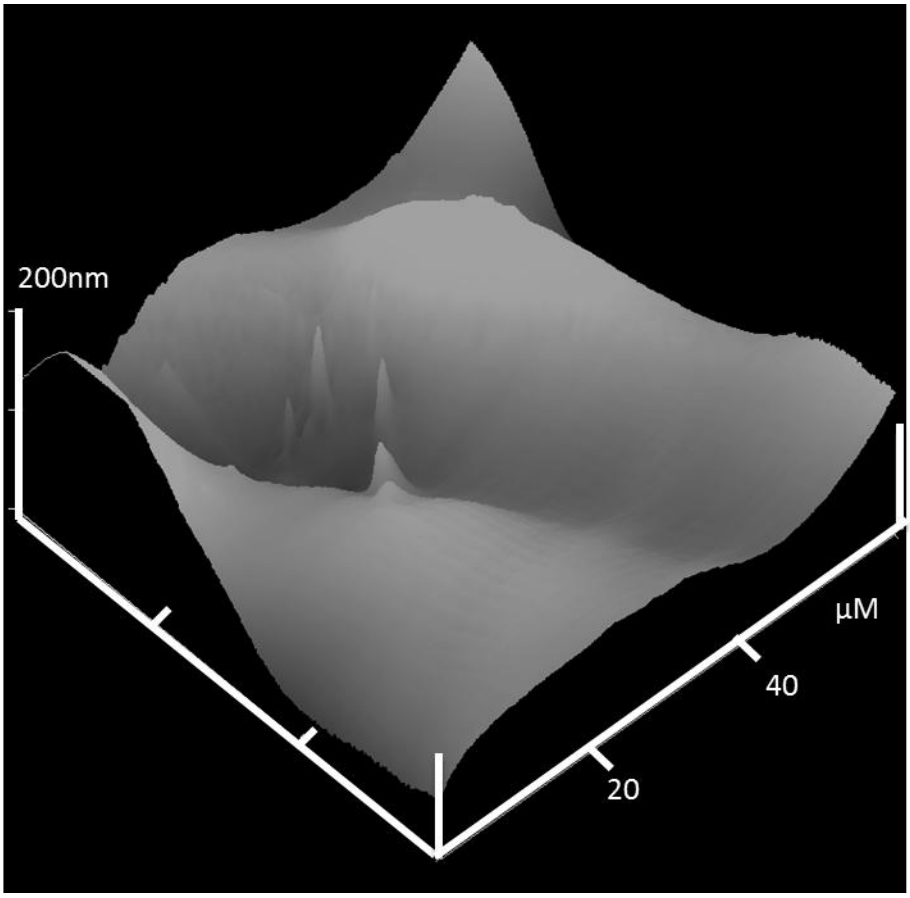

Figure 3.7. Atomic Force microscopy (AFM) of individual BSA_{TETA}/fsDNA molecular assembly fibers (300 µM BSA_{TETA}, 800 µM fsDNA) extracted from glass cover slip after drying 24 hours at room temperature. Samples were placed on mica surface and measured at scan rate of 0.1 Hz.

A.

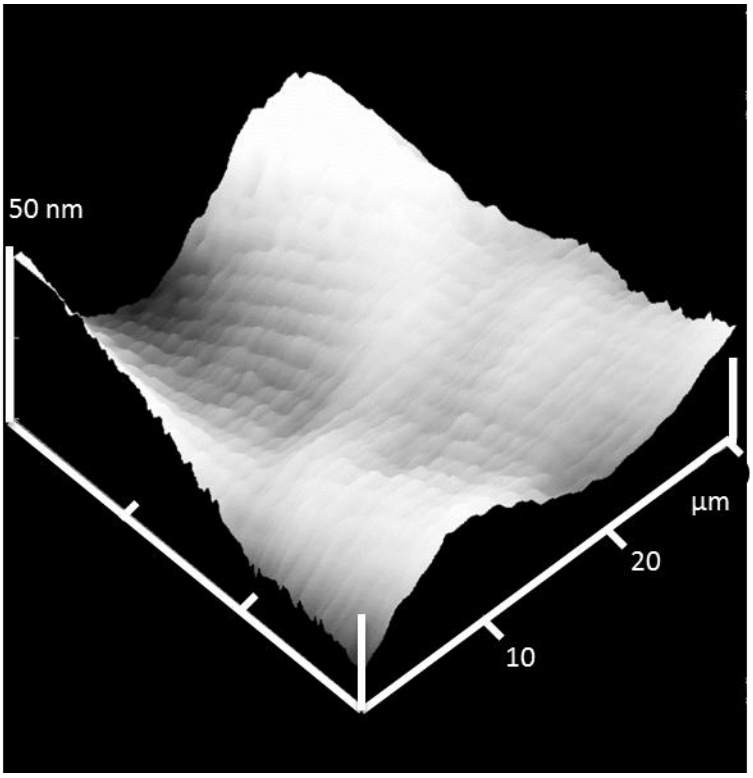

B.

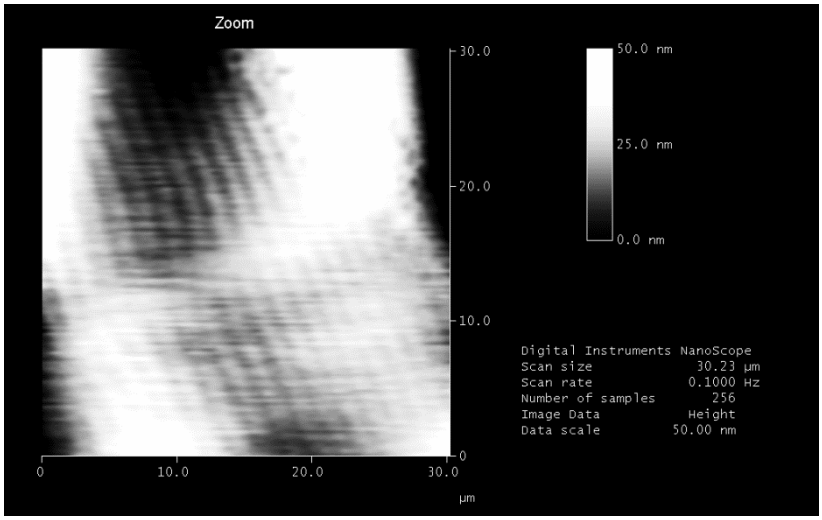

Figure 3.8. AFM micrograph of surface composition of BSA_{TETA}/fsDNA construct zoomed in to analyze fibril-like structures appearing to line surface. Distinct linear fibers corresponding to the lengthwise orientation of larger superstructures can be distinguished.

A.

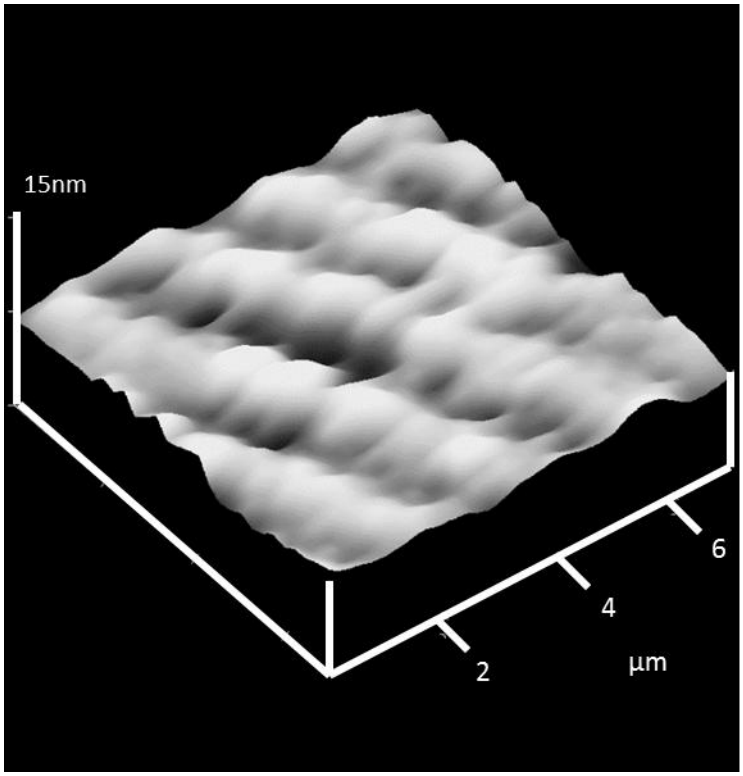

B.

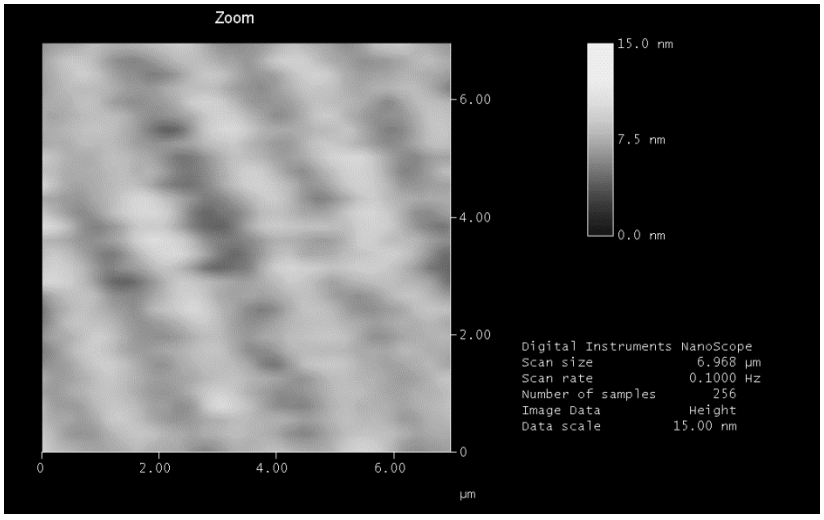

Figure 3.9. AFM micrograph and 2-dimensional profile of enhanced surface morphology of BSA_{TETA}/ fsDNA constructs consisting of dozens of microfibrils with high uniformity and width of ~1.5 µm.

3.3.7 Powder X-Ray Diffraction of BSA_{TETA}/ DNA complex films

To determine the level of crystallinity and order on a macro scale of these molecular assemblies, X-Ray Diffraction was performed to determine the spacing, if any, of these highly ordered samples. There was no peak displaying order or crystallinity to distinguish the BSA_{TETA}/ DNA film from that of the regular glass slide that the film was casted on (**Figure 3.9**). Interestingly, though data shows high levels of uniformity and organization at the level of nanometers and micrometers, XRD data shows that there is no significant organization of the structures at the molecular level, which goes against normal conventional wisdom of assembling structures.

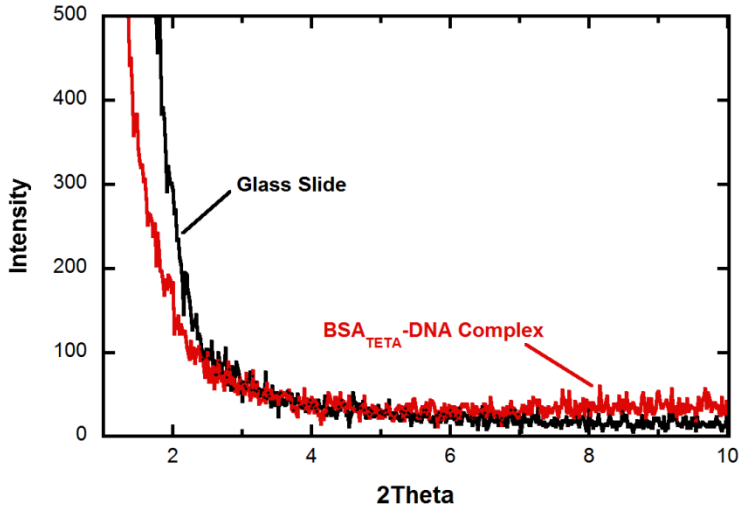

Figure 3.10. Powder X-Ray Diffraction data of molecular assembly when compared with glass slide surface which 300 μM BSA_{TETA}/ 800 μM DNA dissolved in HPLC grade dH_2O was drop-casted on. Data suggests that while molecular assemblies are highly organized on micron scale, there is no discernable ordering or stacking of organized micro-scale structures which compose larger highly organized structures.

3.4 Discussion

Here, we investigated the structure and formation of highly organized BSA_{TETA}-DNA molecular assemblies upon being casted and dried on glass surfaces. The ability of proteins to interact with DNA via electrostatic interactions in solution has been studied by our lab previously in order to construct light harvesting complex by conjugating chromophores to protein-DNA scaffolds. By chemically modifying bovine serum albumin (BSA), a robust globular protein, with poly-amine functional groups, binding to DNA was enhanced due in part to the increase in favorable charge regions between the positively charged surface of the protein and the negatively charged phosphate backbone of DNA. Serendipitously, we have discovered that the molecular morphology of the chemically modified protein-DNA assemblies in the dried film state led to the formation of highly organized, macro-scale structures.

Normally, molecular assemblies arise from small units that become ordered and grow based on entropic favorability or as a seeding unit, like in the case of crystallography. SEM and AFM data shows that the BSA_{TETA}-DNA assemblies are highly organized on the scale of tens and hundreds of microns, while XRD data suggests that there is fundamental disordering at the lower molecular level. This type of contrast to conventional bio-molecular assembly formation raises a multitude of questions when it comes to how the overall macro-scale structures arise. While the imaging capability of the machines used has provided valuable insight into the surface morphology and large scale organization of the structures, little is still known as far as how the structures arise during the film casting process.

One theory as to how the macro-scale structures arise is that the initial protein-DNA interactions provide nucleation sites for the elongation of these large scale structures. As the drying of the film progresses, the concentration of both the DNA and proteins attached to the

long DNA chains increases due to evaporation of solvent. At a critical time-point, enough of the solvent has evaporated so that the surface tension put on the BSA_{TETA}-DNA is great enough to fracture long portions of these assemblies, thereby forming the sharp edged constructs seen in optical microscopy and SEM. The positive charge of the BSA_{TETA} molecules leads to a mimic of histone proteins and can effectively bend and wind the DNA in a supercoiling fashion.

Another analysis of these constructs led to the investigation into the possibility of forming biological heteroepitaxy systems. Epitaxial crystallization occurs when there is growth of a solid in a crystalline phase upon a surface or substrate which is of an equal or different composition.[93, 94] It has been shown in the literature that microscope slides equivalent to those used in our experiments, coated with poly-L-lysine induced selectively controlled tetragonal lysozyme crystals.[95] Due to the similarity in charge and flexibility of TETA to poly-L-lysine, the structures forming on the surface of the glass slide could be due to nucleation sites of protein-DNA complexes that grow due to the length of the DNA polymer chain. SEM imaging in Figure 3.5 shows that in order to obtain the long, highly organized molecular constructs, both the BSA_{TETA} and DNA components are necessary. Individualized, the BSA_{TETA} can form the molecular constructs due most likely to nucleation sites on the glass slide surface, but not the length scale as when DNA is present. DNA on the other hand can form long structures without the chemically modified BSA, but cannot become organized into the block formation observed in the bioconjugate. This leads to the belief that the protein is able to form small clusters of the construct which are further elongated by the presence of DNA connecting individual "blocks" together to form large scale structures.

Interaction of poly-amine sites that are not associated with the oxygen of the DNA phosphate backbone are free to the silica surface of the glass slide lead to large scale formations

of the organized structures that we see. As the volume of the suspension that is casted onto the glass slide decreases, the available solvent that the protein and DNA can interact with diminishes, leading to forced association of the DNA with available protein groups that may have not been bound before. Therefore, the loss of volume of solvent will increase concentration of both BSA_{TETA} and DNA, leading to an enhancement in the binding constant (k_b) of the system.

The binding of BSA_{TETA} is believed to be electrostatically and entropically driven, but it is interesting to note that another factor may be leading to the interesting formation of these molecular assemblies. Triethylenetetramine, used within our group as a quality modifier of protein surface charge to enhance interaction with solids[96] and polymers[97], is also an excellent stabilizer of a parallel G- quadruplex structure upon association of DNA, leading to stabilization of inter- and intra-molecular structures and acting as a transcriptional repressor.[98] Its ability to chelate to Cu^{II} is also known as a treatment of Wilson's disease[99], meaning it is a biologically compatible molecule that has the potential to create larger, organized structures when in the presence of DNA. With an excess of TETA present to bind and form a stable quadruplex with multiple DNA molecules, an explanation as to the large length of these molecules can be presented.

The association between protein biomolecules modified with triethylenetetramine and the DNA strands leads to the primary level of growth. The TETA associates with the DNA electrostatically, forming the aforementioned quadruplex via inter-molecular association. In previous studies we have shown that one modified BSA_{TETA} sample has the potential to interact with DNA on a length scale of ~26 base pairs.[89] As the volume of solvent decreases in the drying process, the number of associations of free modified protein to DNA becomes greater, and it is

possible to increase the rigidity of the DNA due to a wrapping process. As protein interacts with DNA, multiple protein-DNA strands have the potential to also interact via favorable electrostatic interactions. The second level of association then becomes multiple BSA_{TETA} -DNA induced quadruplex structures interacting in order to increase entropy of the system as the volume decreases in the drying process. By the time the volume is nearly completely removed from the system, the interactions of the protein-DNA secondary structures leads to the formation of macro-scale tertiary structures that are visible under optical microscopy. Finally, the intensity of surface tension at the critical point where volume is at a minima leads to fracturing of the tertiary complexes along critical fault points giving rise to the uniform width of the constructs.

3.5 Conclusions

Manipulation of biologically based macromolecules to create functional structures has the potential to revolutionize the way materials are used and manufactured. However, with a myriad of variables needing to be controlled, precise techniques make this aspiration difficult to attain. Mutation of proteins and other types of post translational modification to achieve controllable assembly of dynamic molecules to utilize their diverse molecular functions is an exciting field but hindered by the difficulty in control over these mechanisms.

While attempting to use these protein-DNA constructs for another practical application, we in fact stumbled across an even more complicated and interesting derivative of the project. Highly organized structures between specially modified protein and DNA have been formed due to unexplained parameters that will require further investigation. What is known from these preliminary studies, however, is that there is a unique interaction between the chemically modified protein and the DNA in solution. Characterization down to the micron length shows what appear to be dozens of smaller fibrils, coalescing to create these large structures that are visible to the human eye. Assembly of this degree stemming from a molecular scale that is achievable by facile laboratory techniques has the potential to revolutionize biomaterial fabrication.

This association gives rise to large scale structures that can be used as high surface area reaction centers of biofuel cells, or as channeling directors for studies in Surface Plasmon Resonance, among other applications. In addition, if these bio-molecular assemblies are in fact the product of multiple levels of association between the protein and DNA structures, the tinsel strength of the constructs could be tested and may be incredibly high. These fascinating results are yet another example of how common biological materials can be used in fields of medicine,

manufacturing, and therapeutics to improve on current techniques, and develop a new wave of functional, eco-friendly, bionanomaterials.

References

[1] K. M. Koeller, C. H. Wong, *Nature*. **2001**, *409*, 232-240.

[2] R. L. Schowen, R. L. Gandour, *Transition States of Biochemical Processes*, 1st ed. Plenum, **1978**

[3] P. L Privalov, *Adv. Protein Chem.* **1979**, *33*, 167-241.

[4] F. Hofmeister, *Arch. Expth. Pathol. Pharmakol.* **1888**, *24*, 247.

[5] C. Harriette, C. J. Martin, *J. Physiol.* **1911**, *43*, 1-27.

[6] D. Stigter, D. O. V. Alonso, K. A. Dill, *Proc. Natl. Acad. Sci.* **1991**, *88*, 4176-4180.

[7] S. Basu, S. Sen, *Chem. Inf. And Model.* **2009**, *49*, 1741-1750.

[8] S. S. Strickler, A. V. Gribenko, A. V. Gribenko, T. R. Keiffer, J. Tomlinson, T. Reihle, V. V. Loladze, G. I. Makhatadze, *Biochem*. **2006**, *45*, 2761-2766.

[9] T. J. Magliery, J. J. Lavinder, B. Sullivan, *Curr. Opin. Chem. Biol*. **2011**, *15*, 443-451.

[10] T. Alber, *Annu. Rev. Biochem.* **1989**, *58*, 765-798.

[11] B. Van den Burg, V. G. H. Eijsink, *Curr. Opin. Biotechnol.* **2002**, *13*, 333-337.

[12] Z. Kamal, S. Ahmad, T. R. Molugu, A. Vijayalakshmi, M. V. Deshmukh, R. Sankaranarayanan, N. M. Rao, *J. Mol. Biol.* **2011**, *413*, 726-741.

[13] A. A. Pakula, R. T. Sauer, *Nature*. **1990**. *344*, 363-364.

[14] H. Hamada, T. Arakawa, K. Shirani, *Curr. Phar. Biotechno.* **2009**, *10,* 400-407.

[15] G. DeSantis, J. B. Jones, *Opin. Biotechnol.* **1999**, *10*, 324-330.

[16] K. Polizzi, A. S. Bommarius, J. M. Broering, J. F. Chaparro-Riggers, *Curr. Opin. Chem. Biol.* **2007**, *11*, 220-225.

[17] A. Murphy, C. óFágáin, *Biotechnol.* **1996**, *49*, 163-171.

[18] E. Baslé, N. Joubert, M. Pucheault, *Chem. Biol.* **2010**, *17*, 213-227.

[19] O. A. Roholt, D. Pressman, *Methods Enzymol.* **1972,** *25*, 438-449.

[20] M. Gorbunoff, Cyanuration. *Methods Enzymol.* **1972**, *25*, 506-514

[21] P. E. Wilcox, Esterification. *Methods Enzymol.* **1972**, *25*, 596-615.

[22] B. A. Thomas, L. P. McMahon, A. V. Klotz, *Biochem.* **1995**, *34*, 3758-3770.

[23] I. M. Klotz, Succinylation. *Methods Enzymol.* **1967**, *11*, 576-580.

[24] I. S. Carrico, *Chem. Soc. Rev.* **2008**, *37*, 1423-1431.

[25] C. V. Kumar, M. R. Duff, *J. Am. Chem. Soc.* **2009**, *131*, 16024-16026.

[26] L. Ballel, K. Alink, M. Slijper, C. Versluis, R. M. J. Liskamp, R. J. Pieters, *ChemBioChem.* **2005**, *6*, 291-295.

[27] A. K. Kumagai, J. B. Eisenberg, W. M. Pardridge, *J. Biol. Chem.* **1987**, *262*, 15214-15219.

[28] K. Krikstopaitis, J. Kulys, L. Tetianec, *Electrochem. Comm.* **2004**, *6*, 331-336.

[29] M. J. Roberts, M. D. Bentley, J. M. Harris, *Adv. Drug Deliv. Rev.* **2002**, *54*, 459-476.

[30] J. Futami, M. Kitazoe, H. Murata, H. Yamada, *Expert Opin. Drug Discov.* **2007**, *2*, 261-269.

[31] G. Wohlfahrt, S. Witt, J. Hendle, D. Schomburg, H. M. Kalisz, H. J. Hecht, *Acta Crystallogr.* **1999**, *55*, 969-977.

[32] C. M. Wong, K. H. Wong, X. D. Chen, *Appl. Microbiol. Biotechnol.* **2008**, *78*, 927-938.

[33] D. G. Hoare, D. E. Koshland Jr., *J. Am. Chem. Soc.* **1966**, *88*, 2057-2058.

[34] D. M. Krizek, M. E. Rick, Current Protocols in Cell Biology, Unit 6.7, Wiley Online Library; Johansson, B. G. *Scand. J. Clin. & Lab Invest.* **1972**, *29*, 7-19.

[35] A. Buranaprapuk, S. P. Leach, C. V. Kumar, J. R. Bocarsly, *Biochem. Biophys. Acta.* **1998**, *1387*, 309-316.

[36] C. V. Kumar, A. Chaudhari, *J. Am. Chem. Soc.* **2000**, *122*, 830-837.

[37] D. R. Nelson, A. K. Huggins, *Anal. Biochem.* **1974**, *59*, 46-53.

[38] W. B. Gratzer, D. A. Cowburn, *Nature*. **1969**, *222*, 426-431.

[39] J. W. Bye, R. J. Falconer, *J. Phys. Chem. B.***2014**, IN PRESS

[40] T. Oshima, *Curr. Opin. Struct. Biol.* **1994**, *4*, 623-628.

[41] C. O'Fágáin, *Enzyme Microb. Technol.* **2003**, *33*, 137-149.

[42] Z. Hall, H. Hernández, J. Marsh, S. A. Teichmann, C. V. Robinson, *Structure.* **2013**, *21*, 1325-1337.

[43] T. Kuila, S. Bose, P. Khanra, A. K. Mishra, N. H. Kim, J. H. Lee, *Biosens. Bioelectron.* **2011**, *26*, 4637-4648.

[44] R. Cheng, Y. Liu, S. Ou, Y. Pan, S. Zhang, H. Chen, L. Dai, J. Qu, *Anal. Chem.* **2012**, *84*, 5641-5644.

[45] S. Wu, Q. He, C. Tan, Y. Wang, H. Zhang, *Small* **2013**, *9*, 1160-1172.

[46] L. Chen, B. Wei, X. Zhang, C. Li, *Small* **2013**, *9*, 2331-2340.

[47] L. Bashi, M. Frasconi, R. Tel-Vered, O. Yehezkeli, I. Willner, *Anal. Chem.* **2008**, *80*, 8253-8259.

[48] C. Huang, H. Bai, C. Li, G. Shi, *Chem. Commun.* **2011**, *47*, 4962-4964.

[49] A. Pattammattel, M. Puglia, S. Chakraborty, I. K. Deshapriya, P. K. Dutta, C. V. Kumar, *Langmuir* **2013**, *29*, 15643-15654.

[50] C. Liu, S. Alwarappan, Z. Chen, X. Kong, C.-Z. Li, *Biosens. Bioelectron.* **2010**, *25*, 1829-1833.

[51] H. Shen, M. Liu, H. He, L. Zhang, J. Huang, Y. Chong, J. Dai, Z. Zhang, *J. Appl. Mater. Interfaces* **2012**, *4*, 6317-6323.

[52] K. Yang, L. Feng, X. Shi, Z. Liu, *Chem. Soc. Rev.* **2013**, *42*, 530-547.

[53] C. Chung, Y.-K. Kim, D. Shin, S.-R. Ryoo, B. H. Hong, D.-H. Min, *Acc. Chem. Res.* **2013**, *46*, 2211-2224.

[54] J. Zhang, F. Zhang, H. Yang, X. Huang, H. Liu, J. Zhang, S. Guo, *Langmuir* **2010**, *26*, 6083-6085.

[55] L. Jin, K. Yang, K. Yao, S. Zhang, H. Tao, S.-T. Lee, Z. Liu, R. Peng, *ACS Nano* **2012**, *6*, 4864-4875.

[56] X. Zuo, S. He, D. Li, C. Peng, Q. Huang, S. Song, C. Fan, *Langmuir* **2009**, *26*, 1936-1939.

[57] C. V. Kumar, A. Chaudhari, *Chem. Commun.* **2002**, 2382-2383.

[58] C. V. Kumar, A. Chaudhari, *J. Am. Chem. Soc.* **2000**, *122*, 830-837.

[59] J. M. Sanchez-Ruiz, *Biophys. Chem.* **2010**, *148*, 1-15.

[60] Van den Burg, B.; Eijsink, V. G. H. *Curr. Opin. Biotechnol.* **2002**, *13*, 333-337.

[61] D. Perl, F. X. Schmid, *J. Mol. Biol.* **2001**, *313*, 343-357.

[62] M. Wunderlich, A. Martin, F. X. Schmid, *J. Mol. Biol.* **2005**, *347*, 1063-1076.

[63] W. S. Hummers, R. E. Offeman, *J. Am. Chem. Soc.* **1958**, *80*, 1339-1339.

[64] M. A. Zia, K.-u. Rahman, M. K. Saeed, F. Andaleeb, M. I. Rajoka, M. A. Sheikh, I. A. Khan, A. I. Khan, *Journal of Clinical Biochemistry and Nutrition* **2007**, *41*, 132-138.

[65] G. W. Castellan, *Physical Chemistry*; 2nd Ed.; Addison-Wesley Publishing Co., **1971**, 780-787.

[66] M. D. Gouda, S. A. Singh, A. G. Appu Rao, M. S. Thakur, N. G. Karanth, *J. Biol. Chem.* **2003**, *278*, 24324-24333.

[67] M. S. Akhtar, A. Ahmad, V. Bhakuni, *Biochemistry* **2002**, *41*, 3819-3827.

[68] V. Georgakilas, M. Otyepka, A. B. Bourlinos, V. Chandra, N. Kim, K. C. Kemp, P. Hobza, R. Zboril, K. S. Kim, *Chem. Rev.* **2012**, *112*, 6156-6214.

[69] T. S. Sreeprasad, V. Berry, *Small* **2013**, *9*, 341-350.

[70] K. Yang, Y. Li, X. Tan, R. Peng, Z. Liu, *Small* **2013**, *9*, 1492-1503.

[71] Y. Zhang, J. Zhang, X. Huang, X. Zhou, H. Wu, S. Guo, *Small* **2012**, *8*, 154-159.

[72] Q. Shao, P. Wu, X. Xu, H. Zhang, C. Cai, *PCCP* **2012**, *14*, 9076-9085.

[73] Y. Zhang, C. Wu, S. Guo, J. Zhang, in *Nanotechnology Reviews, Vol. 2*, **2013**, p. 27.

[74] R. E. M. Diederix, M. Ubbink, G. W. Canters, *ChemBioChem* **2002**, *3*, 110-112.

[75] X. Zuo, S. He, D. Li, C. Peng, Q. Huang, S. Song, C. Fan, *Langmuir* **2009**, *26*, 1936-1939.

[76] G. W. Castellan, *Physical Chemistry*; 2nd Ed.; Addison-Wesley Publishing Co., **1971**, 780-787.

[77] J. M. Sanchez-Ruiz, G. I. Makhatadze, *Trends Biotech.* **2001**, *19*, 132-135.

[78] P. Pandey, S. P. Singh, S. K. Arya, V. Gupta, M. Datta, S. Singh, B. D. Malhotra, *Langmuir* **2007**, *23*, 3333-3337.

[79] Johnson, D. S.; Mortazavi, A.; Myers, R. M.; Wold, B. *Science.* **2007**, *316*, 1497- 1502.

[80] M. Ptashne, A. Gann, *Nature.* **1997**, *386*, 569-577.

[81] S. Malik, R. G. Roeder, *Annu. Rev. Genet.* **2000**, *34*, 77-137.

[82] A. L. Olins, D. E. Olins, *Science*. **1974**, *183*, 330-332.

[83] J. M. Pascal, P. J. O'Brien, A. E. Tomkinson, T. Ellenberger, *Nature*. **2004**, *432*, 473-478.

[84] A. T. Fenley, D. A. Adams, A. V. Onufriev, *Biophys. Jour.* **2010**, *99,* 1577-1585.

[85] L. Jen-Jacobson, *Biopolymers*. **1997**, *44*, 153-180.

[86] D. L. Nelson, M. M. Cox, *Lehninger: Principles of Biochemistry*; 6th ed.; W. H. Freeman,

2012.

[87] F. Thoma, T. Koller, A. Klug, *J. Cell Biology*, **1979**, *83*, 403-427.

[88] S. F. Lambert, J. O. Thomas, *Eur. J. Biochem.* **1986**, *160*, 191-201.

[89] C. V. Kumar, M. R. Duff, *J. Am. Chem. Soc.* **2009**, *131*, 16024-16026

[90] J. A. A. W. Elemans, A. E. Rowan, R. J. M. Nolte, *J. Mater. Chem.* **2003**, *13*, 2661-2670.

[91] S. Zhang, *Nature Biotechnology.* **2003**, *21*, 1171-1178.

[92] A. A. Schiller, R. W. Schayer, E. L. Hess, *J. Gen. Physiol.* **1953**, *36*, 489-506.

[93] K. A. Mauritz, E. Baer, A. J. Hoppinger, *J. Polymer Sci.***1978**, *13*, 1-61.

[94] E. I. Givargizov, M. O. Kliya, V. R. Melik-Adamyan, A. I. Grebenko, R. C. DeMattei, R. S. Feigelson, *J. Cryst. Growth Des.* **1991**, *112*, 758-772.

[95] L. Rong, H. Komatsu, M. Natsuisaka, S. Yoda, *JPN. J. Appl. Phys.* **2001**, *40*, 6677-6678.

[96] R. Chowdhury, B. Stromer, B. Pokharel, C. V. Kumar, *Langmuir* **2012**, *28*, 11881-11889.

[97] V. K. Mudhivarthi, K. S. Cole, M. J. Novak, W. Kipphut, I. K. Deshapriya, Y. Zhou, R. M. Kasi, C. V. Kumar, *J. Mater. Chem.* **2012**, *22*, 20423-20433.

[98] F. Yin, J. Liu, X. Deng, J. Wang, *J. Biochem.* **2007**, *141*, 669-674.

[99] J. M. Walshe, *Lancet* **1982**, *1*, 643-647.